

Strangeness Enhancement

Challenges and Successes

Johann Rafelski^a

Department of Physics, University of Arizona, Tucson, AZ 85721

Abstract. Highly effective conversion of kinetic energy into abundant particle multiplicity is the remarkable feature discovered in high energy heavy ion collisions. This short and pedagogic review addresses topical issues related to the understanding of this phenomenon, originating in the creation of the deconfined quark–gluon plasma phase. I consider in depth the apparently simple, yet sometimes misunderstood, intricate issues: a) statistical hadro-chemistry, chemical parameters, b) strange flavor chemical equilibration in quark–gluon plasma, and c) particle yields and sudden hadronization, in the historic perspective of work and competition with my friend József Zimányi.

1 Creation of Matter in Laboratory

Today, we are at the verge of understanding the origin of matter surrounding us. How did visible matter which surrounds us, all the protons and neutrons, i.e., ‘hadrons’ form, emerging from the quark–gluon soup which filled the early Universe? In laboratory experiments involving collisions of large nuclei at relativistic energies, several (nearly) independent reaction steps occur, and ultimately are leading to hadron production:

- 1) formation of the primary fireball; a momentum equipartitioned partonic phase comprising in a limited space-time domain the final state entropy;
- 2) the cooking of the energy content of the hot matter fireball towards the yield (chemical) equilibrium in a hot perturbative quark–gluon plasma phase — this is the quark–gluon plasma liquid (QGP) — a drop of the matter that filled the universe up to about $30\mu\text{s}$;
- 3) emergence near to the phase boundary of *transient* massive effective quarks and disappearance of free gluons; this phase cannot be in chemical equilibrium if entropy, energy, baryon number and strangeness are to be conserved;
- 4) hadronization, that is combination of effective and strongly interacting $u, d, s, \bar{u}, \bar{d}$ and \bar{s} quarks and anti-quarks into the final state hadrons, with the yield probability weighted by accessible phase space.

In particular, the hadronization process can be subject to detailed experimental study, and one of the points of interest is how, as function of increasing energy of colliding nuclei, the hadronization of the dense quark–gluon matter fireball occurs — we argue that at sufficiently high energy, e.g., at RHIC, this happens in a rapid and explosive manner, forcing the global bulk matter into ‘single’ time freeze-out ‘hadronization’. The methods we discuss here should also allow to settle open questions about low energy reactions, i.e., how fast hadronization proceeds at SPS range of energies and if hadrons remain hadrons without quark degrees of freedom appearing in the reaction at all, or perhaps there is an intermediate domain of constituent quark matter. This is the ‘low energy’ heavy ion frontier. The high energy frontier is the arrival

^a e-mail: rafelski@physics.arizona.edu

Dedicated to memory of Prof. József Zimányi

of LHC-CERN heavy ion research program which will allow us to explore the extreme conditions of perturbative quark–gluon plasma. In these notes, we will focus on RHIC and LHC case only.

The abundant production, in these ‘high energy’ heavy ions reactions, of strange flavored hadrons is a direct consequence of the process of chemical equilibration of strange quarks in QGP. In the Summer 1980, I proposed that the strangeness abundance, along with strange antibaryon yields offers an opportunity to identify formation of the deconfined quark–gluon matter, and the exploration of its properties. The original argument as stated at the time follows in the following verbatim [1], since I could not really present it better today¹:

... assuming equilibrium in the quark plasma, we find the density of the strange quarks to be (two spins and three colors)²:

$$\frac{N_s}{V} = \frac{N_{\bar{s}}}{V} = 6 \int \frac{d^3p}{(2\pi)^3} e^{-\sqrt{p^2+m_s^2}/T} = 3 \frac{T m_s^2}{\pi^2} K_2(m_s/T), \quad (1)$$

(neglecting, for the time being, the perturbative corrections and, of course, ignoring weak decays). As the mass of the strange quarks, m_s , in the perturbative vacuum is believed to be of the order of 280–300 MeV³, the assumption of equilibrium for $m_s/T \simeq 2$ indeed correct. In Eq. (1), we were able to use Boltzmann distribution, as the density of strangeness is relatively low. Similarly, there is a certain light anti-quark density (\bar{q} stands for either \bar{u} or \bar{d}):

$$\frac{N_{\bar{q}}}{V} \simeq 6 \int \frac{d^3p}{(2\pi)^3} e^{-|p|/T - \mu_q/T} = e^{-\mu_q/T} T^3 \frac{6}{\pi^2}, \quad (2)$$

where the quark chemical potential is $\mu_q = \mu_B/3$, μ_B is baryochemical potential. This exponent suppresses the $q\bar{q}$ pair production as only for energies higher than μ_q is there a large number of empty states available for the q .

What we intend to show is that there are many more \bar{s} quarks than anti-quarks of each light flavor. Indeed:

$$\frac{N_{\bar{s}}}{N_{\bar{q}}} = \frac{1}{2} \left(\frac{m_s}{T} \right)^2 K_2(m_s/T) e^{\mu_B/(3T)}. \quad (3)$$

The function $x^2 K_2(x)$ is, for example, tabulated in Abramowitz-Stegun. For $x = m_s/T$ between 1.5 and 2, it varies between 1.3 and 1. Thus, we almost always have more \bar{s} than \bar{q} quarks and, in many cases of interest $N_{\bar{s}}/N_{\bar{q}} \simeq 5$. As $\mu_B \rightarrow 0$ there are about as many \bar{u} and \bar{d} quarks as there are \bar{s} quarks.

When the quark matter dissociates into hadrons, some of numerous \bar{s} may, instead of being bound in a $q\bar{s}$ Kaon, enter into a $(\bar{q}\bar{q}\bar{s})$ anti-baryon ...

There are three important issues raised above, which since have seen a long and tedious further development:

1. the chemical equilibration of strange quarks;
2. the combinant quark hadronization;
3. the importance of strange anti-baryons as signature of QGP.

Very few people at first noted our work, let alone evaluate its relevance and validity. However, following several lectures, in particular also at the October 1980 GSI workshop⁴ which was attended by József Zimányi, already by the Summer 1981, Tamás Bíró working with József

¹ Another reason for the verbatim presentation of this text is that no regular publication occurred, and libraries tend to dispose of the old 1980 conference volumes — for this reason a scan of this articles is also available at <http://www.physics.arizona.edu/~rafelski/rare.htm>:

² I changed here the notation $s \rightarrow N_s$, $\bar{s} \rightarrow N_{\bar{s}}$ etc, to correspond to the notation of this presentation.

³ This high value of strange quark mass based on qualitative consideration of hadron spectra, was soon recognized to be a factor two too large, and further underwent a slow but steady reduction as function of time and the development of better analysis methods. Today, value is just about 1/3 as large, an thus assumption of equilibrium in QGP is less of a challenge than it seemed in the year 1980.

⁴ Workshop organized by R. Bock and R. Stock on *Future Relativistic Heavy Ion Experiments* held at GSI-Darmstadt, October 7–10, 1980, in GSI 81-6 report.

Zimányi obtained strangeness production rates in perturbative QCD when considering the specific processes $q\bar{q} \rightarrow s\bar{s}$. The result of this study was that it would take much too long, about 8 times the natural lifespan of a QGP fireball, to equilibrate strangeness chemically. Unfortunately, when József Zimányi came to present these yet preliminary results in Frankfurt in late Summer 1981, I was not aware of this visit set-up on a short notice by my Institute director, Walter Greiner. Upon my return from Seattle, Walter greeted me with the announcement, “Johann, József Zimányi has shown your strange theory could be wrong”. For a young man at the beginning of his career this was quite an event, hard to forget.

Walter has been convinced by the presentation, moreover, he needed my talents for the study of the vacuum in strong fields. As weeks passed, the pressure in Frankfurt increased: Walter argued that I should cease all ‘strange’ quark–gluon activity which, as József Zimányi has shown, could not be right. Finally, I believe in late October 1981, I (and Walter⁵) received a copy of the Biró–Zimányi preprint [2]. For the first time, I saw in any detail the contents of József’s lecture, and I saw an important omission.

Among my CERN-earned credentials 1977–80 was some knowledge about charm production in pp reactions: I shared, for about a year, an office with Brian Combridge, of perturbative QCD charm production fame [3]. I was induced to Hagedorn’s relativistic thermodynamics and statistical bootstrap, and in parallel also, to perturbative QCD charm production. In the fall 1981, this turned out to be a valuable asset. I had learned from Brian that even if the cross sections were similar for both quark $q\bar{q} \rightarrow c\bar{c}$ and gluon $GG \rightarrow c\bar{c}$ fusion processes into charm, it was the gluon which dominated the production rate. Once I saw that $GG \rightarrow s\bar{s}$ was not considered in the Biró–Zimányi preprint, I knew that the essence of the calculation of the strangeness production relaxation time remained open. I described my insight to Walter, who did not like the idea that gluons, at the time very hypothetical objects, would be in essence the cause of strangeness production (a speculative signature) in the quark–gluon plasma, another highly hypothetical object. On the other hand, my colleague Berndt Müller was enthusiastic at the prospect to use real gluons in a physical process. We had just completed a study based on virtual gluon fluctuations of the temperature dependence of the latent heat of the QCD Vacuum [4], and thus the glue based flavor producing reactions did not seem exotic at all given this preparation.

Within a few days of work, we found that indeed the thermal strangeness chemical equilibrium in quark–gluon plasma is due to gluon fusion process [5]. The issue of chemical equilibration in QGP became an asset, for QGP chemical equilibrium yield of strangeness evolved into an indicator of the presence of mobile, free gluons, and thus of deconfinement: The work of Biró–Zimányi showed that as long as there was no free glue, just light u, \bar{u}, d, \bar{d} quarks, chemical equilibration was not attainable. This was elaborated for the physical case of a hadron gas in a kinetic approach by another talented student, Peter Koch. He computed the strangeness yields and relaxation times expected in the hadron phase [6,7]. By 1986, Strangeness yield enhancement has been well established theoretically as signature for deconfinement, and the strength of this enhancement was recognized to depend on how long the hot QGP phase would last.

An important aspect in the evaluation of the rate of strangeness production, which Berndt and I undertook, was the choice of the value of the running strong coupling constant $\alpha_s(\Lambda)$. We knew very well that if one uses a 1st-order perturbative expression for a QCD process, it can only produce reasonable results if the coupling strength is chosen at the right strength for the energy scale. We studied the results available and decided that the right α_s value to produce strangeness at the typical thermal collision energy, $\Lambda \simeq 3\text{--}6T$, for $T = 200\text{--}300$ MeV should be $\langle\alpha_s\rangle = 0.6$. This turned out to be just the right choice, as later precision measurements of α_s have shown⁶. Yet, for the following 15 years, a value $\langle\alpha_s\rangle = 0.2$ was often used in literature, and our results were not, in general, trusted — however, this smaller value is appropriate for the energy scale $\Lambda \simeq 6$ GeV, beyond the energy scales where thermal strangeness production is occurring.

⁵ Walter’s copy was in my mailbox marked: \Rightarrow Rafelski: *Johann, bitte Rücksprache darüber!* Walter

⁶ The particle data group links to a web page where one can enter the reaction energy scale and gets back the strength of the QCD coupling, see <http://www-theory.lbl.gov/~ianh/alpha/alpha.html>, the value $\alpha_s(0.86\text{GeV}) = 0.60 \pm 0.10 \pm 0.07$ is obtained.

It is important to recognize that reaction rates grow with α_s^2 , hence using $\langle\alpha_s\rangle = 0.2$ instead of $\langle\alpha_s\rangle = 0.6$ one finds a relaxation time which is longer by an order of magnitude. While we predicted $\tau \simeq 2\text{fm}/c$, I saw also results as large as $15\text{ fm}/c$. An uninvolved observer could not readily recognize that this was simply a consequence of a different and seen from historic perspective wrong choice of the QCD interaction strength. Indeed, I even had the impression that the authors of these papers did not see that their results differed mostly and nearly only due to different choice of the coupling strength. About the same time, α_s^2 was measured precisely, and first systematic study of strangeness enhancement appeared; a rapid shift of opinion ensued following the Warsaw ICHEP⁷ conference in 1996. Despite this, still today, more than 10 years later some confusion about strangeness chemical equilibration lingers on. To set the record straight, let us clearly state that:

- a) at RHIC-200 it is the QGP phase which equilibrates chemically,
- b) produced hadron abundances are determined by the QGP hadronization process.

It is important to note that these results are independently a consequence of both, theoretical analysis based on known fundamental properties of strong interactions, and an analysis of experimental data. Considering the totality of RHIC results pointing to rapid, nearly instantaneous hadronization, and early parton thermalization, I see no path leading to the chemical equilibrium among hadrons produced. The remainder of this paper will lay foundation for understanding of this situation.

2 Statistical Hadronization

Since the beginning of the friendly science competition I have had with József Zimányi and his group, much of our effort was devoted to the understanding of how exactly production of hadrons occurs, and the methods we developed are similar, with the overriding element being the conservation of energy, flavor and consideration of entropy so that it cannot decrease in the recombinant mechanisms.

The Budapest group obtained the hadron multiplicities within the framework of the algebraic coalescence re-hadronization model (ALCOR) [8], not much different of my efforts. However, my focus at the time was to develop methods of diagnosis of the QGP using specifically strange particle production [7,9], from which emerged the Fermi-2000 hadron production model (for a review, see [10]). An elaboration of this effort is the SHARE (Statistical HAdronization with REsonances) suite of programs [11,12]. We find that the overall hadronic particle yields are well described by the statistical hadronization model (SHM), a point made by several other groups as well [13], including features of the hadron spectra.

The SHM is an elaboration of the Fermi model of hadron formation, based on the hypothesis that the strong interactions saturate the quantum particle production matrix elements. Therefore, the yield of particles is controlled primarily by the accessible phase space, and not by reaction strength. In the original Fermi model, the accessible phase space is considered in terms of the available energy. We refer to this approach as ‘micro-canonical’. Given the large energy contents of the fireball we use the (grand) canonical approach, with a temperature-like parameter T . The SHM contains little if any information about the nature of interactions, and thus it embodies the principle of reaching simplicity in many body dynamics, allowing to identify the properties of the dense and hot primary matter formed in heavy ion collisions.

2.1 Chemistry parameters explained

We now consider either the phase space into which particles are emitted, or, possibly the actual properties of the hot matter, such as QGP, or even hadron gas, that is a phase of interacting confined hadrons. The objective is to understand how to describe the yields of the multitude of different hadrons emerging.

⁷ See proceedings of the 28th International Conference on High Energy Physics, July 25 – 31, 1996, Z. Ajduk and A.K. Wróblewski, Editors, World Scientific, Singapore.

Each of the hadrons produced will have some quantum numbers such as baryon number, strangeness, etc. which need to be followed and conserved in the reactions. An direct way to accomplish this objective consists in characterizing each particle by the valance quark content and the related quantum numbers [14], we shall establish the relation between valance quark count and the hadron properties below.

In principle, the yield of each particle is governed, aside of other statistical parameters such as the size of the system (volume V) and the (chemical) freeze-out temperature T , by the particle fugacity obtained, as we shall argue, forming a product of two types of chemical factors,

$$\mathcal{Y}_i \equiv \lambda_i^{\pm 1} \gamma_i = e^{\sigma_i^{\pm}/T}, \quad (4)$$

where σ_i^{\pm} is ‘ i ’-particle (antiparticle for lower sign) chemical potential σ_i^{\pm} . We see that for each related particle and antiparticle, we have a different value of \mathcal{Y}_i and thus, if we wish so, of particle chemical potential ($= T \ln \mathcal{Y}_i$). Our approach, i.e., use of γ_i and λ_i is convenient for the control of the difference, and the sum of particles and antiparticles separately as we shall explain just below. Our way of handling chemistry is in principle not different from the ALCOR approach [8], in which two independent chemical potentials for quarks and antiquarks are used. For two reasons, we believe that this way is better; the book-keeping of multitude of particles is easier, and the interpretation of the factors in a microscopic model has the advantage of relating them directly to different type of microscopic reactions.

Thus, in our approach, there are two types of chemical factors γ_i and λ_i . These factors are related to two types of chemical equilibrium, which can be better understood when one introduces γ_i, λ_i as defined above. These are described in table 1. Moreover, there is considerable difference in the dynamics of the (chemical) reaction associated with these parameters, even though, in principle, there is no difference in their fundamental origin and function. To understand better this somewhat special situation, let us focus on strangeness in the hadronic gas phase. The two principal chemical processes are seen in Fig. 1. The redistribution of strangeness among (in this example) Λ , π and N , K seen on left in Fig. 1, constitutes approach to the ‘relative’ chemical equilibrium of these species. In this equilibration process, the available quarks are distributed among hadrons. The picture refers to a typical reaction in which, e.g., $\Lambda + \pi \leftrightarrow N + K$. The s, \bar{s} pair production process, on right in Fig. 1, is responsible for absolute chemical equilibrium of strangeness. Achievement of the absolute equilibrium, $\gamma \rightarrow 1$, require more rarely occurring collisions with annihilation and creation of new (strange) particle pairs, e.g., $N + \pi \leftrightarrow \Lambda + K$. These reactions are ‘OZI’ forbidden, which means that the cross sections are about a factor 10–20 weaker compared to the exchange processes, and thus they are slower in driving the ‘absolute’ chemical equilibrium.

Table 1. Four quarks s, \bar{s}, q, \bar{q} require four chemical parameters; right: name of the associated chemical equilibrium.

λ_i	controls ‘nett’ i.e. difference yield quarks $_i$ – anti-quarks $_i$ ($i = q, s$)	Relative chemical equilibrium
γ_i	controls overall abundance of quark $_i$ ($i = q, s$) pairs	Absolute chemical equilibrium

As a first example, let us illustrate why λ controls the difference between particle and antiparticle number, and γ counts in effect the yield of particle and antiparticle pairs. To see this, let us look at the simple but artificial case of a gas of nucleons and anti-nucleons N, \bar{N} . The two chemical fugacities are:

$$\mathcal{Y}_N = \gamma_N e^{\mu_N/T}, \quad \mathcal{Y}_{\bar{N}} = \gamma_N e^{-\mu_N/T}. \quad (5)$$

Thus, we find for the potentials:

$$\sigma_N \equiv \mu_N + T \ln \gamma_N, \quad \sigma_{\bar{N}} \equiv -\mu_N + T \ln \gamma_N. \quad (6)$$

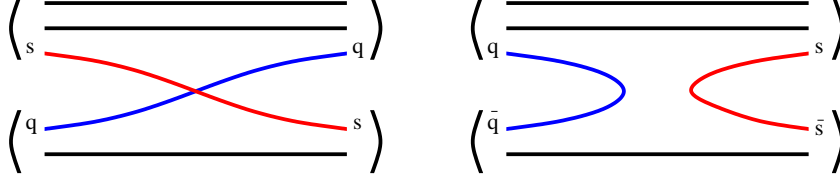


Fig. 1. Typical strangeness exchange (left) and production (right) reactions in the hadronic gas phase.

Considering the first law of thermodynamics:

$$\begin{aligned} dE + P dV - T dS &= \sigma_N dN + \sigma_{\bar{N}} d\bar{N}, \\ &= \mu_N (dN - d\bar{N}) + T \ln \gamma_N (dN + d\bar{N}), \end{aligned} \quad (7)$$

we recognize that the nucleon chemical potential μ_N controls the net nucleon number arising from the particle difference, while γ_N , which we call the phase space occupancy (of nucleons), regulates the number of nucleon–antinucleon pairs present.

In the next example, we consider how we use the quark parameters when dealing with hadrons. Noting the valance quark content, of $p(ud)$, $\bar{p}(\bar{u}\bar{d})$, we have

$$\mathcal{R}_p = (\gamma_u^2 \gamma_d) (\lambda_u^2 \lambda_d) \quad \mathcal{R}_{\bar{p}} = (\gamma_u^2 \gamma_d) (\lambda_u^{-2} \lambda_d^{-1}), \quad (8)$$

and thus we can write:

$$\mathcal{R}_p = \gamma_u^2 \gamma_d e^{\frac{2\mu_u + \mu_d}{T}} = \gamma_B e^{\frac{\mu_B}{T}}, \quad \mathcal{R}_{\bar{p}} = \gamma_u^2 \gamma_d e^{\frac{-2\mu_u - \mu_d}{T}} = \gamma_B e^{\frac{-\mu_B}{T}}. \quad (9)$$

In case of $\Lambda(uds)$, $\bar{\Lambda}(\bar{u}\bar{d}\bar{s})$, we need to respect an important historical anomaly, i.e., negative S-strangeness assignment to s -hadrons, e.g.:

$$\mathcal{R}_\Lambda = \gamma_u \gamma_d \gamma_s e^{\frac{\mu_u + \mu_d + \mu_s}{T}} = \frac{\gamma_B}{\gamma_S} e^{\frac{\mu_B - \mu_S}{T}}, \quad \mathcal{R}_{\bar{\Lambda}} = \gamma_u \gamma_d \gamma_s e^{\frac{-\mu_u - \mu_d - \mu_s}{T}} = \frac{\gamma_B}{\gamma_S} e^{\frac{-\mu_B + \mu_S}{T}}. \quad (10)$$

This anomaly was the historical reason why we (I and all my collaborators) in general follow quark flavor and use quark chemical factors to minimize the confusion arising. There is a second reason, as we shall see just below. First, in order to focus on the important parameters, and considering the good symmetry between u and d quarks, we simplify notation, allowing us to refer generically to the light quarks q :

$$\lambda_q \equiv \sqrt{\lambda_u \lambda_d}, \quad \mu_q = \frac{\mu_u + \mu_d}{2}; \quad \lambda_{I3} \equiv \sqrt{\frac{\lambda_u}{\lambda_d}}, \quad \mu_{I3} = \frac{\mu_u - \mu_d}{2}. \quad (11)$$

and similarly for γ_q and γ_{I3} .

We thus now can write for the above examples of p which we call generically $N(qqq)$ for nucleon, Λ which we call generically $Y(qqs)$, adding further the case of double-strange $\Xi(qss)$:

$$\begin{aligned} \mathcal{R}_N &= \gamma_q^3 e^{\frac{3\mu_q}{T}} = \gamma_B e^{\frac{\mu_B}{T}}, & \mathcal{R}_{\bar{N}} &= \gamma_q^3 e^{\frac{-3\mu_q}{T}} = \gamma_B e^{\frac{-\mu_B}{T}}, \\ \mathcal{R}_Y &= \gamma_q^2 \gamma_s e^{\frac{2\mu_q + \mu_s}{T}} = \frac{\gamma_B}{\gamma_S} e^{\frac{\mu_B - \mu_S}{T}}, & \mathcal{R}_{\bar{Y}} &= \gamma_q^2 \gamma_s e^{\frac{-2\mu_q - \mu_s}{T}} = \frac{\gamma_B}{\gamma_S} e^{\frac{-\mu_B + \mu_S}{T}}, \\ \mathcal{R}_\Xi &= \gamma_q \gamma_s^2 e^{\frac{\mu_q + 2\mu_s}{T}} = \frac{\gamma_B}{\gamma_S^2} e^{\frac{\mu_B - 2\mu_S}{T}}, & \mathcal{R}_{\bar{\Xi}} &= \gamma_q \gamma_s^2 e^{\frac{-\mu_q - 2\mu_s}{T}} = \frac{\gamma_B}{\gamma_S^2} e^{\frac{-\mu_B + 2\mu_S}{T}}. \end{aligned} \quad (12)$$

Naturally, I can write similar equations for the Ω and $\bar{\Omega}$, kaons, and all strange particles in general.

The second historical anomaly is that we recognize in above relations that, in order to relate the quark and hadron quantum numbers, there is only one choice:

$$\mu_B = 3\mu_q, \mu_S = \mu_q - \mu_s; \quad \mu_q = \frac{1}{3}\mu_B, \mu_s = \frac{1}{3}\mu_B - \mu_S. \quad (13)$$

To make the 2nd anomaly explicit: these relations seem to imply that there is no baryon number in the strange quarks! μ_s does not enter into the magnitude of μ_B . One can trace this anomaly to the assignment of the full baryon number to Y , Ξ along with ‘strangeness’ $S = -1$ and -2 quantum numbers respectively. Thus, even though strange quarks contain baryon number they are counted as being ‘baryon-free’ when it comes to hadronic chemistry based on historic definitions.

These two anomalies have lead, as I have seen it over 25 years, to a few cases of confusion. Thus let me offer instruction on how you can check published results without doing a complete re-computation — this task is easy for baryons. One notices that:

$$\left(\frac{\bar{\Lambda}}{\Lambda}\right) / \left(\frac{\bar{p}}{p}\right) = \left(\frac{\bar{\Xi}}{\Xi}\right) / \left(\frac{\bar{\Lambda}}{\Lambda}\right) = \left(\frac{\bar{\Omega}}{\Omega}\right) / \left(\frac{\bar{\Xi}}{\Xi}\right) = e^{+2\mu_S/T}. \quad (14)$$

When I read a paper, I first check these relations! In fact they must be true also for microscopic codes which do quark coalescence, since the particle specific factors cancel, and the equality must be correct to all significant figures, since a potential error can be confined excited baryon states used in the evaluation of the final yields. I note that sometimes there is a correction, when λ_{I3} are allowed to vary from unity, in order to account for the slight up/down quark number asymmetry. In that case, recall to replace above $\bar{p}/p \rightarrow \lambda_{I3}^2 \bar{p}/p$ and $\bar{\Xi}/\Xi \rightarrow \lambda_{I3}^{-2} \bar{\Xi}/\Xi$.

In the third example, consider the question, what does it mean to say that strangeness in QGP is in chemical equilibrium? In the QGP, at sufficiently high temperature, the density of strangeness flavor is described by the Fermi distributions:

$$\langle \frac{N_s}{V} \rangle = \langle \rho_s \rangle = \int \frac{d^3p}{(2\pi)^3} \frac{1}{\lambda_s^{-1} \gamma_s^{-1} e^{E(p)/T} + 1}, \quad \langle \frac{N_{\bar{s}}}{V} \rangle = \langle \rho_{\bar{s}} \rangle = \int \frac{d^3p}{(2\pi)^3} \frac{1}{\lambda_s \gamma_s^{-1} e^{E(p)/T} + 1}. \quad (15)$$

Since strangeness is produced in pairs, the number of strange quarks $\langle s \rangle$ is equal to that of strange anti-quarks $\langle \bar{s} \rangle$, and thus the QGP strangeness fugacity $\lambda_s = 1$. Said differently, when local strangeness density is balancing, the strange quark chemical potential $\mu_s = T \ln \lambda = 0$. On the other hand, the phase space occupancy parameter γ_s is at the QGP formation small, though non-zero since there is direct production of strangeness in pre-thermal parton collisions. Thereafter, strangeness yield grows and at high temperature where Boltzmann approximation is very precise,

$$\gamma_s \simeq \frac{\rho_s + \rho_{\bar{s}}}{\rho_s^{\text{eq}} + \rho_{\bar{s}}^{\text{eq}}}. \quad (16)$$

To recapitulate, when pair production processes are possible, the hadro-chemistry is greatly simplified by the introduction of the phase space occupancy parameter γ_i which controls the abundance of pairs of particles of type i . In many reaction environments, the absolute chemical equilibrium distribution $\gamma_i = 1$ is reached, at which entropy is maximized. In general, the value of γ_i results from dynamical development of the reaction. It is not customary to introduce a chemical potential associated with the occupancy fugacity γ_i since the change in γ_I is not due to chemical processes, but is solely due to particle pair production. On the other hand, the conventional chemical potentials describe relative yields of particles and reflect the properties of the medium, for example in baryon rich matter there is an asymmetry in the yield of charged kaons, with the yield of $K^+(u\bar{s}) > K^-(\bar{u}d)$. In the deconfined phase, in order to conserve entropy the dimensionless quantity $\mu_B/T = 3\mu_q/T$ is nearly conserved in hydrodynamic expansion of QGP. This means that μ_q, μ_B evolves in time along with T .

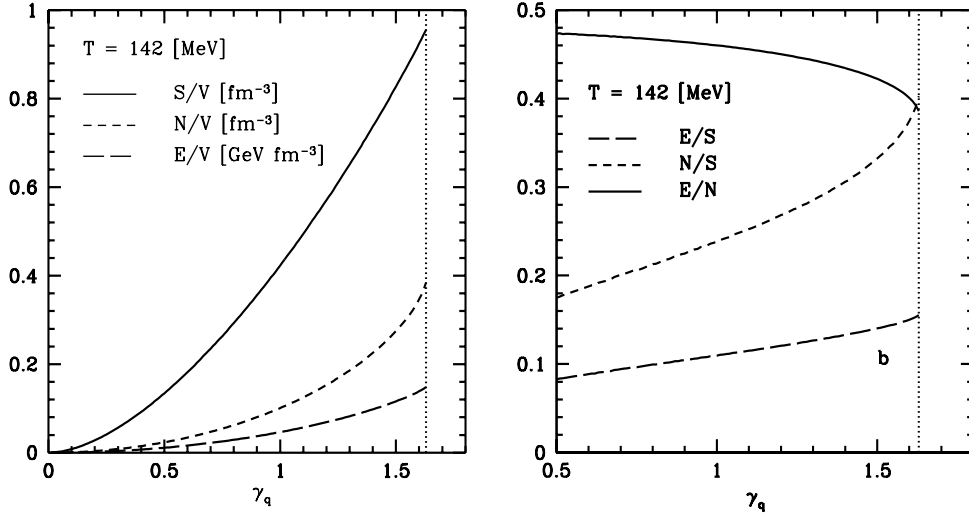


Fig. 2. Entropy density S/V along with particle density N/V and energy density E/V as function of γ_q at $T = 142$ MeV. Ratios of these quantities are shown on right.

2.2 Entropy must increase, strangeness is conserved in hadronization

The microscopic process leading to the hadronization of QGP phase is not understood. However, several observables such as pion correlations, suggest that hadrons are emerging within a very short time from a relatively small space-time volume domain [15,16]. In this process, hadron formation has to absorb the high entropy content of QGP which originates in broken color bonds. The lightest hadron is pion and most entropy per energy is consumed in hadronization by producing these particles abundantly. The particle number, and the entropy content follows from Eq. (18):

$$S_\pi = \int \frac{d^3p d^3x}{(2\pi\hbar)^3} [(1 + f_\pi) \ln(1 + f_\pi) - f_\pi \ln f_\pi], \quad f_\pi = \frac{1}{\gamma_q^{-2} e^{\sqrt{m_\pi^2 + p^2}/T} - 1}. \quad (17)$$

As is seen in⁸ Fig. 2, the maximum entropy density S/V occurs for an over-saturated pion gas, $\gamma_q \simeq e^{m_\pi/2T} \simeq 1.6$. Here, the entropy density of such a saturated Bose gas is twice as large as that of chemically equilibrated Bose gas. Since aside of pions also many other hadrons are produced, the large value of γ_q is necessary and sufficient to allow for the smooth in μ_B, T and V transformation of a QGP into hadrons. The number of active degrees of freedom in the over-saturated hadron gas with $\gamma_q \rightarrow \gamma_q^{\max}$ and in ‘freezing’ QGP phase is very similar.

We used, in Eq. (17), a form which contains in an explicit way the non-equilibrium occupancy parameter. This can be justified noticing that the maximization of micro-canonical entropy,

$$S_{F,B} = \int \frac{d^3p d^3x}{(2\pi\hbar)^3} \mp [(1 \mp f_{F,B}) \ln(1 \mp f_{F,B}) - f_{F,B} \ln f_{F,B}], \quad (18)$$

(where indeed minus sign is for fermions and plus sign for bosons) subject to energy and particle (e.g., baryon, flavor, etc.) number conservation implies the quantum distributions [17]:

$$\frac{d^6 N_i}{d^3p d^3x} = \frac{g_i}{(2\pi)^3} \frac{1}{\gamma_i^{-1} e^{E_i/T} \pm 1}, \quad \gamma_i^{\text{bosons}} \leq e^{m_i/T}. \quad (19)$$

⁸ I use this opportunity to point out that in earlier versions of this figure, I have used a normalization appropriate for gluons, rather than pions, and hence the different densities displayed on left have considerably smaller normalization, while the ratios on the right are in essence unchanged.

When the phase space is not densely occupied, the term ± 1 in the denominator can be neglected and we have the commonly used Boltzmann approximation:

$$\frac{d^6 N_i}{d^3 p d^3 x} = g_i \frac{\mathcal{Y}_i}{(2\pi)^3} e^{-E_i/T}. \quad (20)$$

In Eq. (19), for the Boson distribution, the value of \mathcal{Y}_i is limited in magnitude by the Bose condensation singularity. This singularity presents a limit on the maximum value of the fugacity, for example for pions we have:

$$\mathcal{Y}_\pi \leq e^{m_\pi/T} \equiv (\gamma_q^{\max})^2. \quad (21)$$

This plays a very pivotal role considering that the mass of the pion and the hadronization temperature are similar. Large value of $\gamma_q \rightarrow e^{m_\pi/2T}$ can be directly noticed in pion spectra in an up-tilt in the soft portion of the m_\perp distribution. A similar constraint is also arising for γ_s but it is much less restrictive given the higher mass of the strangeness. Only in exceptional circumstance this could be of physical interest. A more detailed study shows that most significant constraint arises from consideration of the η which condenses for $\gamma_s \rightarrow 10.4$ [18].

We can now compare to the entropy content of the deconfined QGP state. At sufficiently high temperature the entropy density S/V is that of ideal quark-gluon gas:

$$\frac{S}{V} = \frac{4\pi^2}{90} g(T) T^3 = \text{Const.}, \quad (22)$$

where we consider the quark and gluon degrees of freedom along with their QCD corrections, extrapolating the entropy in QGP fitted to the lattice equations of state :

$$g = 2_s 8_c \left(1 - \frac{15\alpha_s(T)}{4\pi} + \dots \right) + \frac{7}{4} 2_s 3_c n_f \left(1 - \frac{50\alpha_s(T)}{21\pi} + \dots \right). \quad (23)$$

The number of quark flavors is $n_f \simeq 2 + \gamma_s 0.5z^2 K_2(z)$, where $z = m_s/T$. The terms proportional to chemical potentials are not shown in the expression for entropy, since $\mu/\pi T \ll 1$ at RHIC and LHC.

Remarkably, the different temperature dependent corrections cancel, and one finds that it is possible to use a nearly T independent value for the effective degeneracy, $g \simeq 30$ near to QGP breakup condition, which value is decreasing to $g \simeq 28$ for equilibrated QGP near $T = 260$ MeV [19]. This is a relatively large number comparing to a pion gas. However, aside of pions the hadron phase has many other particles and resonances and one finds, in a quantitative evaluation, the value of γ_q for which at a given volume (fixed in sudden hadronization) the entropy is equal for both states. The (critical) value $\gamma_q = 1.4$ is found for $T \simeq 140$ MeV, decreasing with increasing temperature and crossing $\gamma_q = 1$ at $T \simeq 180$ MeV.

Thus, in fast hadronization of the QGP phase without an increase in volume, we expect that when entropy is conserved, the value of γ_q would be greater than unity for every value of T considered in previous studies of the hadronization process, with the relation being approximately:

$$\gamma_q \simeq 1.6 - 0.015(T - 140) [\text{MeV}] \quad (24)$$

We are further able to evaluate the magnitude of γ_s/γ_q after hadronization, assuming that at RHIC and LHC the QGP phase is nearly chemically equilibrated at point of hadronization. The strangeness and entropy content when carried across the phase boundary is seen to in essence create a one-to-one functional relationship. For more detail, we refer to recent work of Ms. Inga Kuznetsova [19], seen in Fig. 3. We recognize that at LHC where strangeness can be even over saturated, with the ratio of strangeness pair number to entropy reaching 0.04 (see section 3.4), we expect $\gamma_s/\gamma_q > 2$. This will create an interesting challenge, which I wish József Zimányi could be part of.

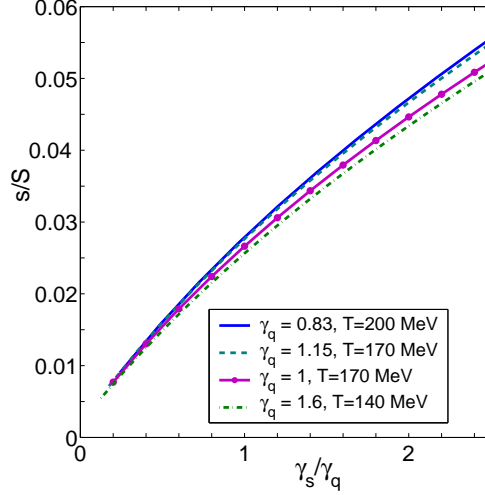


Fig. 3. (color on line) Strangeness to entropy ratio, s/S , as a function of γ_s/γ_q . (solid line, blue) for $T = 200$ MeV, $S^H = S^Q \rightarrow \gamma_q = 0.83$; (dashed line, blue) for $T = 170$ MeV, $S^H = S^Q \rightarrow \gamma_q = 1.15$; (dash-dotted line, green) for $T = 140$ MeV, $S^H = S^Q \rightarrow \gamma_q = 1.6$; (dot marked solid, violet) for $\gamma_q = 1, T = 170$.

3 Strangeness production 25 years after

3.1 Strangeness per entropy

The total final state hadron multiplicity is a measure of the entropy S produced. In the QGP, the entropy production occurs predominantly early on in the collision during the parton thermalization phase. Once a quasi-thermal exponential energy distribution of partons has been formed, the entropy production has been completed. Since the kinetic processes leading to strangeness production are slower than the parton equilibration process, we are rather certain that the production of entropy occurs mainly prior to strangeness production [20]. However, strangeness production by gluon fusion is most effective in the early, high temperature environment, and it continues to act during the evolution of the hot deconfined phase until hadronization.

Our study of the thermal strange particle production processes is based on kinetic theory of particle collisions. While the degree of chemical equilibration of gluons in early stages (which dominate strangeness production) are uncertain, we find that, in particular, the observable ‘strangeness per entropy’ N_s/S (also colloquially referred to as s/S) is insensitive to this uncertainty. This insensitivity expresses the fact that at a given entropy content the temperature can be high at low particle yield, or vice-versa, we can have large number of particles at low temperature. In the cumulative strangeness production process, these effects compensate, as we shall here illustrate, and the final strangeness yield is not initial state dependent (i.e., not dependent on full gluon equilibration).

Both strangeness and entropy are nearly conserved near, and at hadronization, and thus the final state hadronic yield analysis which measures, using the produced particle multiplicities, the value of the final state s/S , is closely related to the thermal processes in the fireball at $\tau \simeq 1\text{--}4$ fm/c. In fact, I can estimate the magnitude of s/S in the QGP phase, considering the hot early stage of the reaction. For an equilibrated QGP phase with perturbative properties, we have discussed above:

$$\frac{s}{S} \equiv \frac{\rho_s}{S/V} \simeq \frac{(\gamma_s(t)g_s/\pi^2)T^3 0.5 x^2 K_2(x)}{g 4\pi^2/90 T^3} = \frac{\gamma_s g_s}{g} 0.23[0.5 x^2 K_2(x)]. \quad (25)$$

For early times, when $x = m_s/T(t)$ is relatively small, the equilibrium value ($\gamma_s = 1$) can be as large as $s/S \simeq 0.045$. However, at high temperature strangeness is not yet equilibrated

chemically. For $m_s/T \simeq 0.7$ appropriate for hadronization stage, the QGP chemical equilibrium is reached when $s/S \simeq 0.041$. We will see, in section 3.4, that this value is fully achieved at LHC, while at RHIC we expect to be 10-15% below chemical equilibrium in QGP.

To close this discussion, I note that consideration of the production of strangeness at a fixed temperature T , and not at a fixed entropy S , is not advisable, as this frees the outcome from an important experiment related constraint, and it is easy to claim that strangeness will not equilibrate in QGP. I observe here that, when the initial temperature is reduced by 20%, the initial entropy content is cut in half. This means that there are half as many gluons, and the rate of strangeness production by gluon fusion is cut down by a factor 4. For this reason, we will look at how the specific yield s/S evolves, and, along with this, at the chemical equilibration achieved in QGP.

3.2 Strangeness production

The kinetic evolution of strangeness in the local (co-moving) frame of reference, the rate of change of strangeness, is due to production and annihilation reactions only:

$$\frac{1}{V} \frac{dN_s}{d\tau} = \frac{1}{V} \frac{dN_{\bar{s}}}{d\tau} = \frac{1}{2} \rho_g^2(t) \langle \sigma v \rangle_T^{gg \rightarrow s\bar{s}} + \rho_q(t) \rho_{\bar{q}}(t) \langle \sigma \rangle_T^{q\bar{q} \rightarrow s\bar{s}} - \rho_s(t) \rho_{\bar{s}}(t) \langle \sigma v \rangle_T^{s\bar{s} \rightarrow gg, q\bar{q}}. \quad (26)$$

The thermally average cross sections are:

$$\langle \sigma v_{\text{rel}} \rangle_T \equiv \frac{\int d^3p_1 \int d^3p_2 \sigma_{12} v_{12} f(\mathbf{p}_1, T) f(\mathbf{p}_2, T)}{\int d^3p_1 \int d^3p_2 f(\mathbf{p}_1, T) f(\mathbf{p}_2, T)}. \quad (27)$$

$f(\mathbf{p}_i, T)$ are the relativistic Boltzmann/Jüttner distributions of two colliding particles $i = 1, 2$ of momentum p_i , characterized by local statistical parameters.

The temporal evolution of s/S , in an expanding plasma, is governed by:

$$\frac{d}{d\tau} \frac{N_s}{S} = \frac{A^{gg \rightarrow s\bar{s}}}{(S/V)} [\gamma_g^2(\tau) - \gamma_s^2(\tau)] + \frac{A^{q\bar{q} \rightarrow s\bar{s}}}{(S/V)} [\gamma_q^2(\tau) - \gamma_s^2(\tau)]. \quad (28)$$

When all $\gamma_i \rightarrow 1$, the Boltzmann collision term vanishes, and equilibrium has been reached. Here, we use the invariant rate per unit time and volume, $A^{12 \rightarrow 34}$, by incorporating the chemical equilibrium densities into the thermally averaged cross sections:

$$A^{12 \rightarrow 34} \equiv \frac{1}{1 + \delta_{1,2}} \gamma_1 \gamma_2 \rho_1^\infty \rho_2^\infty \langle \sigma_s v_{12} \rangle_T^{12 \rightarrow 34}. \quad (29)$$

$\delta_{1,2} = 1$ for the reacting particles being identical bosons, and otherwise, $\delta_{1,2} = 0$. γ_i expresses the deviation from equilibrium of density ρ_i . Note also that the evolution for s and \bar{s} in proper time of the co-moving volume element is identical as both change in pairs.

3.3 QCD parameters

We evaluate $A^{gg \rightarrow s\bar{s}}$ and $A^{q\bar{q} \rightarrow s\bar{s}}$ employing the available strength of the QCD coupling, and range of accepted strange quark masses. The known properties of QCD strongly constrain our results, however, it turns out that the range of strange quark masses remains sufficiently wide to impact the results. We employ $m_s(\mu = 2 \text{ GeV}) = 0.10 \text{ GeV}$ which remains uncertain at the level of 25%. We compute rate of reactions employing a running strange quark mass working in two loops, and using as the energy scale the CM-reaction energy $\mu \simeq \sqrt{s}$. Since the running of mass involves a multiplicative factor, the uncertainty in the mass value discussed above is the same for all values of μ . Some simplification is further achieved by taking, at temperature T , the value $\mu \simeq 2\pi T$ which is the preferred value of the thermal field theory, and agrees with

the value obtained for the reaction energy in strangeness producing processes. This means that we use $m_s(T) = m_s(\mu = 2\pi T)$ with $m_s(T = 318 \text{ MeV}) = 0.1 \text{ GeV}$.

The strength of the QCD coupling constant is today better understood. We use as reference value $\alpha_s(\mu = m_{Z^0}) = 0.118$, and evolve the value to applicable energy domain μ by using two loops. The behavior of $\alpha_s(\mu)$ explains why it makes sense to use perturbative methods of QCD to describe strangeness production, a relatively soft process: given the magnitude $\alpha_s(\mu = m_{Z^0}) = 0.118$, one can quite well run α_s to the scale of interest, $\mu > 1.2 \text{ GeV}$. The strength of the interaction remains $\alpha_s < 0.5$. In passing, we note that had the strength of $\alpha_s(\mu = m_{Z^0})$ been 15% greater, strangeness production could not be studied in perturbative approach. We can express $\alpha_s(\mu)$ as function of temperature by the conditions $\alpha_s(T) = \alpha_s(\mu = 2\pi T)$. This leads to the expression:

$$\alpha_s(T) \simeq \frac{\alpha_s(T_c)}{1 + C \ln(T/T_c)}, \quad T < 6T_c, \quad (30)$$

with $C = 0.760 \pm 0.002$, $\alpha_s(T_c) = 0.50 \pm 0.04$ at $T_c = 0.16 \text{ GeV}$. We stress that Eq. (30) is a parametrization. Only one logarithm needs to be used to describe the two loop running with sufficient precision, since the range we consider is rather limited, $0.9T_c < T < 6T_c$.

In the presented results for strangeness production, we introduce a multiplicative factor $K = 1.7$, describing the difference between the leading and higher order cross sections. In our case this K -factor accounts for processes odd in power of α_s , such as gluon fusion into strangeness, with gluon bremsstrahlung emitted by one of the strange quarks. These processes cannot be accounted for in a study of scale dependence of the coupling strength, and strange quark mass. Being distinguishable, ‘even’ and ‘odd’ terms are contributing incoherently, always increasing the production rate. The magnitude of K , as required here, has not been computed, the rough magnitude is estimated based on perturbative QCD Drell-Yan lepton pair production[21], and heavy quark production [22].

3.4 Achievement of chemical equilibrium in QGP

An important question is how the value of the unknown initial conditions enters. We have studied this in depth in several different model approaches. The answer ‘practically no dependence’ is best illustrated in the figure 4, where we show using a schematic volume expansion model geared to work for RHIC on left, and on right for LHC. We explore a wide range of initial gluon (and quark) occupancy γ_g , which is shown in the middle panel by dashed lines, the initial values we consider for glue occupancy vary as $0.1 < \gamma_g(\tau_0) < 2.1$ in step of 0.5.

With $\gamma_g(\tau_0)$, we also vary $\gamma_q(\tau_0)$, which following the same functional temporal evolution starting with $2/3$ smaller initial value and evolving 1.5 times slower. Note also that the scale, in top panel, varies between RHIC and LHC cases: the dashed lines denote $2m_s$ on left, and $5m_s$ on right. We use the (initial) value of $N_s/S = 0.016$ and $dS/dy = 5,000$ for RHIC and, respectively $N_s/S = 0.016$ and $dS/dy = 20,000$ for LHC. We see a corresponding variation in T_0 (top panel, left end of solid lines) and γ_s (left end of solid lines in middle panel). The final results for $\gamma_s(\tau_f)$ (right end of solid lines in middle panel) and $N_s(\tau_f)/S$ (bottom panel) are impressively insensitive to this rather exorbitant diversity of initial conditions at fixed entropy content. The spread in $N_s/S(\tau)$ we see in the bottom panel could be seen as a wide line width. We also observe that the reaction processes which change yield of strangeness can compete with the fast $v_\perp > 0.5c$ expansion of QGP only for $T > 220 \text{ MeV}$, for lower temperatures the strange quark yields practically do not change (strange quark chemical freeze-out temperature in QGP).

We learn that strangeness cannot probe the very initial QGP conditions near τ_0 — the memory of the initial history of the reaction is lost, the system is opaque for $\tau < 2\text{--}3 \text{ fm}/c$ to the strangeness signature. On the other hand, and most importantly, for the study here undertaken, this also means that the experimental observables emerging in the break-up of the fireball are characteristic of the properties of nearly chemically equilibrated QGP phase, with some over-saturation expected at LHC due to the continued expansion of QGP after freeze-out of strangeness yield, as is seen on right in Fig. 4, where values $N_s/S \simeq 0.4 > N_s/S|_{\text{eq}}$ are seen.

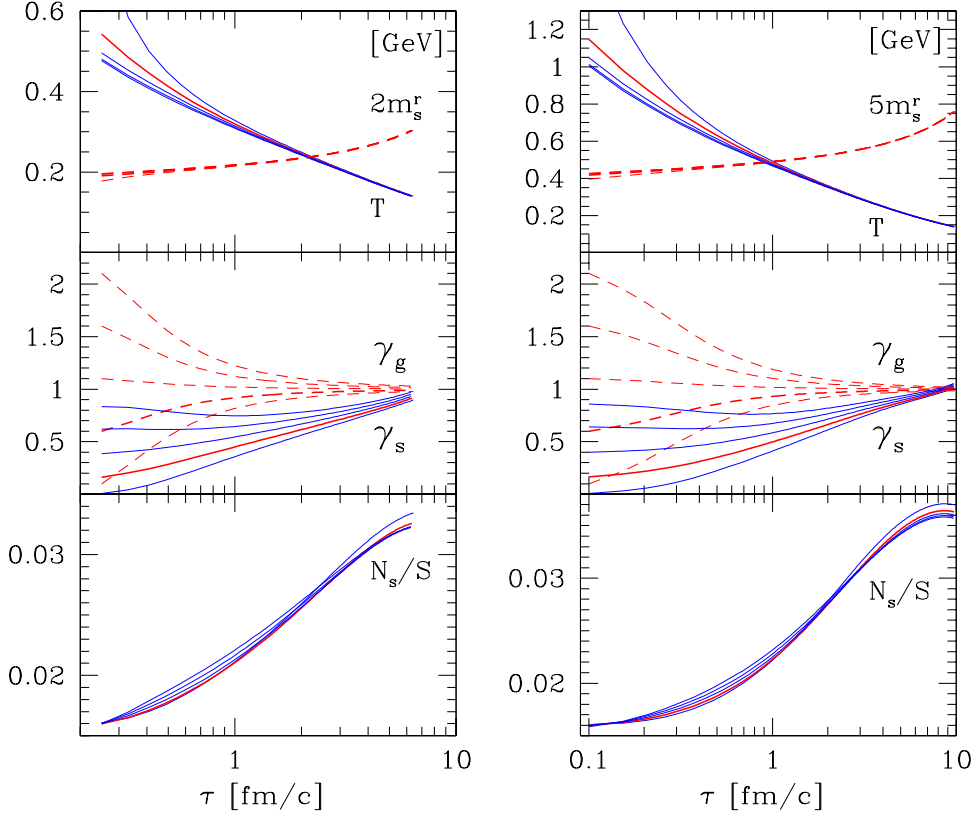


Fig. 4. (color online) RHIC (left) and LHC (right) strangeness production as function of fireball proper time. Volume geometric expansion for most central 5% collisions is assumed. Top panels show the evolution of temperature T and of strange quark mass $m_s(T)$. Middle panel the assumed variation in gluon γ_g (dashed lines), allowed greatly different initial conditions. Solid lines, middle panel, show the resulting γ_s , and in the bottom panel the resulting N_s/S .

A very interesting aspect of the kinetic evaluation of strangeness production is that given the value of s/S in QGP, we are able to evaluate the magnitude of γ_s/γ_q after hadronization, to be expected at LHC, as we did at the end of section 2.2.

3.5 Is strangeness enhancement evidence for QGP?

3.5.1 Overall strangeness

What is exactly “strangeness production enhancement”. To what can we compare? in this report strangeness enhancement refers to a comparison of properties of two matter phases. The first step was the insight that chemically equilibrated QGP has a greater (specific) strangeness content than can be found in the hadron phase space. Responding to the challenge from József Zimányi I found that this high yield is achievable considering QGP based thermal scattering reactions, in which thermally equilibrated perturbative QCD quanta collide. On the other hand similar kinetic calculations show that one cannot expect chemical equilibrium in HG, that is, unless QGP phase acts as catalyst of strangeness formation.

Even in the present theoretical study one must avoid comparing apples and oranges. Comparing the two phases I assure that conserved quantities are the same, such as entropy or baryon number. Whenever all particles produced can be detected, I prefer to relate strangeness enhancement to the number of baryon participants. On the other hand when as at RHIC there

is limited phase space coverage, I must compare strangeness yield in a fixed window of (central) rapidity: ds/dy at a given hadron multiplicity, thus entropy dS/dy . It is very fortunate that even though entropy is itself enhanced by QGP phase formation, strangeness is more enhanced.

At RHIC central rapidity strangeness per entropy (hadron multiplicity) $(ds/dy)/(dS/dy)$ ratio is the observable which can be explored as a function of reaction energy dependence (strangeness excitation function) and centrality dependence. However, this observable is hard to evaluate precisely, many particles need to be measured in same conditions and data analyzed in depth to fill acceptance gaps in kinematic and particle type domains. Thus to report how big the enhancement is, some effort is needed. On the other hand an enhancement of $(ds/dy)/(dS/dy)$ by 40% is a huge effect, very well visible, skewing the general behavior of particle yields towards strange hadrons.

I think all agree and it is quite evident that there are many more strange hadrons made in AA reactions than could be expected in 1980. For example, at central rapidity for the top RHIC energy, there are as many hyperons as there are non-strange baryons. In the lower energy domain at SPS, there is a significant increase in the K^+/π^+ ratio, when comparing NN with AA reactions. A cascade of NN reactions under predicts strangeness yields in presence of QGP, and to meet this challenge new physics is introduced if one wants to avoid QGP but overcome strangeness production blocking in confined phase by high reaction energy thresholds. After 27 years of study AA reactions clearly show the systematic features of strangeness enhancement. Moreover, since there is aside of total strangeness also multistrange hadrons, we have a rich and diverse observable.

3.5.2 Comparing NN and AA individual particle yields

For NN reaction models multistrange hadrons remain an insurmountable challenge. The QGP benefits from the high strangeness density which helps to form multistrange hadrons in the final state. However, in order to be able to speak of enhancement of individual hadrons, such as ϕ or $\bar{\Omega}$ it is necessary to generate a prediction of what the yield would be in absence of quark-gluon plasma. One way to proceed is to compare the yields of these particles originating in chemically equilibrated QGP and HG phases. This than is simply γ_s^n , where n is the strangeness content, and $\gamma_s > 1$ is computed such that the high QGP yield is found in the HG phase. This is the point I made in Ref.[23].

Experimental groups have come to believe that a better measure of enhancement is a comparison of AA yield to NN or NB reactions (where $B \ll A$) at the same nucleon-nucleon reaction energy, and this measure of experimental enhancement has been widely accepted. However, this concept is, like the “theoretical enhancement” I have described above at least in part based on a theoretical model scaling factor [24,25,26], which describes how the *reference* yield should increase if the AA collisions were a series of *independent* NN reactions. The excess over and above this scaling is reported to be due to physics beyond NN interactions. Thus this “experimental enhancement” is ‘gauged’ by this scaling model.

While the Glauber-Bialas scaling is proved by experience in many other environments, there is no way I can see how to confirm experimentally this model input for RHI strange particle production. For this reason when comparing yields in AA with NN reaction other measures of enhancement need to be also thought about. For example we can ask by how much the multistrange hadrons are enhanced as compared to single strange hadrons, since in such double ratio the scaling factor drops out. In a more qualitative statement, one simply observes, that the enhancement of multistrange hadrons with greater strangeness content is greater. In any case the “theoretical” enhancement as proposed in 1982 must not be forgotten, since if it is, one can fall into a trap, that the enhancement arising in the comparison of AA with NN reaction could be also argued to arise from NN strangeness yield suppression. Let us next see how confusion can arise.

3.5.3 In search of a transforming discovery

Many relativistic heavy ion physicists after long years of hard work, are longing for a big discovery. They imagine that the heavy ion collision experiments reached some revolutionary form of matter, so new that we are almost blind to it. An example which challenges such fantasy is that within a factor of two or so the yields of most hadrons is in chemical equilibrium. This behavior seems extraordinary and many of my colleagues are deeply impressed. As I discussed this result is confirming phase space dominance of hadron production and the Fermi statistical model. The phase space dominance picture arises naturally in evaporation of QGP in the process we call hadronization.

On the other hand it could be that there are mechanisms leading to phase space dominance other than QGP. For example it has been suggested that the yield of hadrons in AA reactions is always formed in hadron phase chemical equilibrium, in analogy to the Unruh-Hawking effect) radiation of a small black hole. The Hawking radiation temperature is inversely proportional to the mass of Black-Hole;

$$T_{\text{BH}} = \frac{1}{8\pi GM} = \frac{a}{2\pi} \quad (31)$$

where G is the gravitational constant and M the mass of the black hole, and a the acceleration. The second form relates the Hawking effect to the Unruh effect.

In order to reach hadronic values of T one must in this picture re-think confinement as being due, or simply said, being an event horizon. In that case, by dimensional analysis and/or some wishful thinking [27]:

$$G^2 \propto \frac{1}{M_{\text{Planck}}^4} \rightarrow \frac{1}{32\pi m_h^2 \sigma} \quad (32)$$

where m_h is hadron scale (GeV) mass, and σ is the quark string tension. Clearly, I have somehow to assure universality of primary hadronization temperature: somehow just the right confinement-holes need to be produced reproducibly. So I claim that this is so since the hadron scale m_h is fixed by an extra dimension. In that way we could view $m_h^2 \sigma \rightarrow \rho$ where ρ is the quark-stretch energy in 1+2 dimensions (three regular space less two transverse dimensions + two extra sub-space dimensions). ρ thus has energy density dimension. Equipped with the proper factor it must have as scale the usual 1 GeV/fm³.

So summarize, QCD is to be forgotten, there is some unknown dynamics which expresses itself as Hawking-type radiation emanating from reduced spatial and subspace dimensions. In this picture particle production is computable given the evaporation temperature of the “confinement-hole”, there is no particle production dynamics. Equilibrium is in fact always “natural”. However, temperature of the spectra and yields could be still a function of size/mass scales, that is subspace dimensionality, and the ideas about chemical freeze-out, thermal freeze-out and matter flow will need to be converted into this new language – black-hole-confinement picture reduces dimensionality in normal space and requires extra dimension to compensate this, replacing phase transition temperature by extra dimension structured vacuum properties. Ockham razor edge principle, that is simple is beautiful, says that this is not the right way to proceed.

3.5.4 Canonical strangeness suppression

For this reason let us only retain for the moment the outcome of this, and postulate ab-initio chemical equilibrium for all reactions. If that were true, it is the AA particle yield which is the reference, the variation of particle production I called strangeness enhancement is now strangeness production suppression in NN reactions. To make sure nobody misunderstands: in this sub-sub-section there is 20 fold suppression of Ω production in NN reactions, and accordingly of other particles [28].

Naively one would think that this NN suppression should be explained by a kinetic particle production model. However this is not fitting the approach with ad-hoc assumption of chemical equilibrium for the AA particle yield. It seems on first sight that NN reaction volume being

small, the chemical equilibrium particle yields are to be computed in canonical rather than grand-canonical statistical ensemble. The particle-antiparticle correlation implemented within canonical statistical approach [29] produce naturally a much reduced yields. However the scale of large volume is reached when $Rm > 1$ which in hadronic world is almost always the case, and thus the transition from canonical to grand canonical picture for chemical equilibrium yields occurs for volumes of hadron size. Moreover the yields are very sensitive to the choice of the volume size scale R . This then requires an additional correlation parameter to smooth the R dependence if the ad-hoc assumption of chemical equilibrium is to work [30].

Given the high sensitivity to the volume size of canonical suppression in NN reactions one can produce the required enhancement to AA volume, which qualitatively also describes the hierarchy of single, double and triple strange hadron suppression within (large) error. Note that both AA and NN yields depend sensitively on volume and freeze-out temperature, thus there are at least 4 relevant parameters (two volumes and two temperatures for AA and NN systems), and more refined models introduce additional correlation length parameters. All these can be fine tuned to describe single, double and triple strange hadron suppression and overall hadron yield within the considerable data error.

However, all those pursuing this type of ad-hoc-chemical-equilibrium data interpretation are asking that the QCD practitioners forget about the dynamical particle production work of past 40 years. Instead we apply the hypothesis that some novel, and not yet understood mechanism provides a chemical equilibrium yield, and introduce many parameters to describe the data. Ockham razor edge principle also suggests that this is a wrong approach. However, in perspective of recent history, what invalidated this ‘canonical’ model was not its obvious nonsensical general frame of thought, but the simple fact that something that stands on the head (in terms of enhancement becoming suppression) will end having a wrong centrality and energy dependence [31,32,33].

a) *centrality* dependence: the experimental data for the enhancement show a soft dependence on the reaction volume originating in the slight advantage in kinetic-thermal strangeness production due to prolonged lifespan and greater initial compression for more central (head-on) reactions. This is incompatible with the high sensitivity, nearly threshold behavior of the canonical suppression mechanism:

b) *reaction energy* dependence: the experimental enhancement of multistrange hadron production is nearly the same at top SPS energy and at RHIC.. This is so since in the conventional reaction picture both NN and AA yields rise modestly, for different reasons but in a comparable measure. However, in the canonical model as the reaction energy increases, the NN reaction volume increases in order to absorb all that energy into the system (since T is fixed) , and thus the micro-canonical suppression changes rapidly comparing SPS and RHIC.

4 Where we are with Strangeness and QGP

4.1 Statistical and sudden hadronization

4.1.1 Resonances and Statistical Hadronization

To make a quantitative SHM model of particle production, we must deal with strong interactions among particles, this is done by way of introducing hadron resonances, as Hagedorn has proposed [34]. While resonances are expression of the ongoing collisions and interactions between hadrons, we also need to account for hadron resonance yield when considering the stable hadron yields. One has to be sure to include all the hadronic resonances which decay feeding into the yield considered, e.g., the decay $K^* \rightarrow K + \pi$ feeds into K and π yields. The contribution is sensitive to production temperature at which these particles are formed.

Inclusion of the numerous resonances constitutes a book keeping challenge in study of particle multiplicities, since decays are contributing at the 50% level to practically all particle yields, Fig. 5. A public statistical hadronization program, SHARE has simplified this task considerably [11,12].

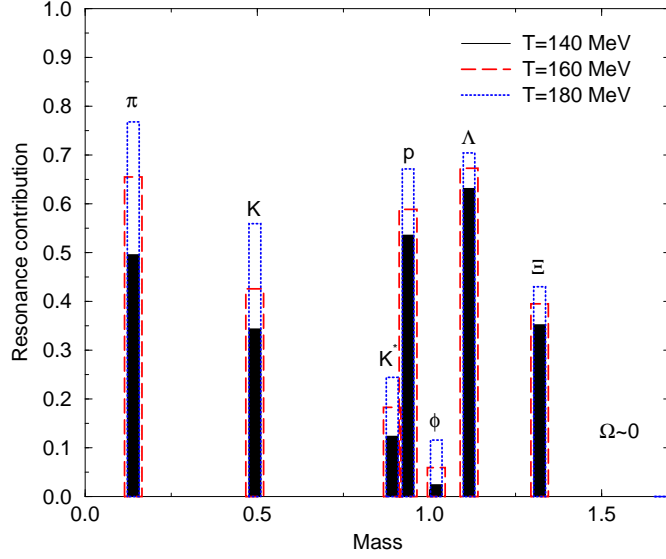


Fig. 5. Relative resonances contribution to the yields of individual stable hadrons for three particle freeze-out temperatures.

We see that the resonance decay contribution is dominant for the case for the pion yield. This happens even though each pion producing resonance contributes relatively little in the final count. However, the sum of small contributions competes with the direct pion yield. On the other hand, for other, more heavy hadrons, generally there is a dominant contribution from just a few, or even from a single resonance. The exception are the Ω , $\overline{\Omega}$ which have no known low mass resonances: the reason is that the ground state has spin 3/2 and the particle being all strange does not have isospin resonances.

We see that except for a few particles most stable hadrons are comprising the yields of a few main sources which, in general, are of comparable magnitude. Inclusion of resonances, thus, is a vital element in any proper description of a hadronic system. This also implies that we can use resonances to test SHM and conversely, without understanding the resonance yields, SHM is meaningless.

The initial test of statistical hadronization approach to particle production is that within a particle ‘family’, particle yields with same valance quark content are in relation to each other thermally equilibrated. Thus, the relative yield of, e.g., $K^*(\bar{s}q)$ and $K(\bar{s}q)$ or Δ and N is controlled only by the particle masses m_i , statistical weights (degeneracy) g_i and the hadronization temperature T . In the Boltzmann limit, one has (star denotes the resonance):

$$\frac{N^*}{N} = \frac{g^* m^{*2} K_2(m^*/T)}{g m^2 K_2(m/T)}. \quad (33)$$

Validity of this relation implies insensitivity of the quantum matrix element governing the coalescence-fragmentation production of particles to intrinsic structure (parity, spin, isospin), and particle mass. The measurement of the relative yield of hadron resonances is a sensitive test of the statistical hadronization hypothesis.

However, the method available to measure resonance yields depends in its accuracy on how sudden the hadronization process is. The observed yield is derived by reconstruction of the invariant mass of the resonance from decay products energies E_i and momenta p_i , specifically: $m^{*2} = (E_1 + E_2)^2 - (\mathbf{p}_1 + \mathbf{p}_2)^2$. Thus, should the decay products of resonances rescatter on other particles after their formation, their energies and momenta will change and normally the invariant mass will not fall into the acceptance bin given by the known mass of the resonance. Hence, not all produced resonances can be, in general, reconstructed. The rescattering effect

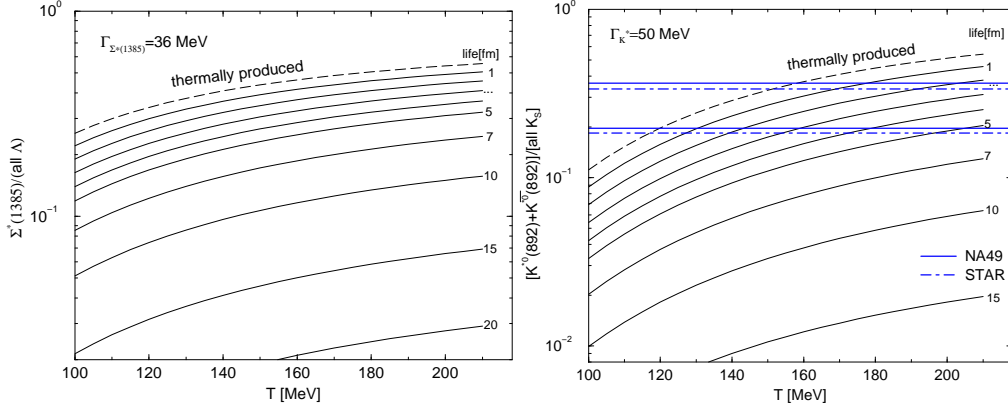


Fig. 6. Observable relative resonance yields as a function of temperature for a given ‘life span’ of interacting hadron gas phase.

depletes more strongly the yields of shorter lived states. These decay sooner and are thus more within the dense matter envelope of the fireball.

To see how this works, we first evaluate the ratios of $(K^* + \bar{K}^*)/K_S$ and $\Sigma^*(1385)/\Lambda$ using SHM [35,36]. The upper dashed lines in Fig. 6 show the result as function of T . In both cases, chemical potential corrections are negligible since the particle’s chemical composition is the same:

$$\frac{N^*}{N + N^*} = \frac{n(m^*, T)}{n(m^*, T) + n(m, T)}, \quad n(m, T) \propto m^2 T K_2\left(\frac{m}{T}\right). \quad (34)$$

To account for the effect of rescattering, we note that after the resonances decay characterized by the width Γ , the decay products undergo rescattering at a rate proportional to the medium’s density as well as the average rescattering rate. The population time evolution (master) equations then are:

$$\frac{dN^*}{dt} = -\Gamma N^* + R, \quad \frac{dD}{dt} = \Gamma N^* - D \sum_j \langle \sigma_{Dj} v_{Dj} \rangle \rho_j \left(\frac{R_0}{R_0 + vt} \right)^3. \quad (35)$$

where the resonance yield is N^* and ‘daughter’ yield is D . v is the expansion velocity, R_0 is the hadronization radius, $\rho_j = n_j(m_j, T)$ the initial hadron gas particle density and $\langle \sigma_{Dj} v_{Dj} \rangle$ is the particle specific thermal average of interaction cross-section multiplied with relative velocity. When $vt \simeq R_0$ the scattering stops, thus qualitatively $R_0/v \simeq \tau c$ is the time of rescattering shown in Fig. 6.

In Eq. (35), the regeneration term R is not relevant since regeneration reaction rates are considerably smaller than scattering rates, and as we shall see, the predicted lifespan of the system is extremely short. However, if and when a long lived system were to emerge, regeneration could be of relevance [37]. Figure 6 shows how the observed ratios of Σ^*/Λ and K^*/K are depleted with varying hadronization time within this model. The main feature of these results is that a ‘high’ resonance yield is signaling a short duration of rescattering and thus of process of hadronization.

As indicated in the figure, and more generally, in summary of the many experimental results now reported [38,39,40] the observed yields are relatively large, showing that there is no suppression of the observed yield for most, if not all, of the resonances observed at RHIC — a somewhat ‘suspect’ yield, is that of $\Lambda(1520)$. It appears to be low comparing $\Lambda(1520)/\Lambda$ -ratio seen in AA reactions with those seen in pp reactions — and thus, we have considered the possibility that this seemingly stable $\Lambda(1520)$ state is in fact a fragile, easily quenched D-wave, just like a quasi-stable ns -wave of an atom [35]. It turns out that as has been the good tradition, József Zimányi, this time working with Peter Levai came across a very similar idea, seeking the effect in the bound state structure which is highly unusual [41]. Potentially, this and other high

mass negative parity resonances could be produced in a coalescence process, with production probability well below the saturation limit required in the SHM model. Because of the high mass, their overall expected yield is sufficiently small, so that this suppression will not alter the global SHM particle production pattern.

The story does not end at this point. Namely, a further explanation we came to realize when working in quantitative fashion with RHIC data is in fact, the most natural one: the fast expansion of the QGP with supercooling. The AA yields are governed, in that case, by QGP hadronization temperature which can be noticeably lower than the temperature-like parameter governing pp reactions freeze-out, and the reduced relative yield of massive resonances is a signature of low freeze-out temperature [42]. Indeed, there has been historically a considerable theoretical bias towards supercooled [43], and thus sudden [44], hadronization, beginning with evaluation of recombinant hadron production [7], and culminating in the usual Zimányi–Rafelski friendly competition, in the study of expanding QGP with confinement considered [45] leading to supercooling [46]. At this time, the conclusion is that either the low hadronization temperature suppresses the heavy resonances and thus helps to find the true hadron yields in SHM, or that some of the resonances are suppressed by hadron structure consideration in violation of SHM model, in which case their yields do not follow the expectations based on Eq. (33). Clearly, study of resonance production is of key importance in understanding heavy-ion collision physics.

4.1.2 Particle yields and hadrochemistry

In order to find the magnitude of the parameters governing the chemical freeze-out, we analyze particle yields and ratios in terms of the chemical parameters and the temperature. Except for direct pions, practically always one can use Boltzmann approximation and large reaction volume, and what follows in this subsection assumes that this simple situation applies. The chemical factors play often the dominant role in understanding these yields.

In order to gain understanding of the chemistry parameters and to understand which particle yields are responsible for which results, it is often appropriate to study (multi) ratios of particle yields as these can be chosen such that certain physical features can be isolated. For example, just the two ratios,

$$R_\Lambda = \frac{\bar{\Lambda} + \bar{\Sigma}^0 + \bar{\Sigma}^* + \dots}{\Lambda + \Sigma^0 + \Sigma^* + \dots} \simeq \frac{\bar{s}\bar{u}\bar{d}}{sud} = \lambda_s^{-2}(\lambda_u\lambda_d)^{-2} = e^{2\mu_S/T} e^{-2\mu_B/T}, \quad (36)$$

$$R_\Xi = \frac{\bar{\Xi}^- + \bar{\Xi}^* + \dots}{\Xi^- + \Xi^* + \dots} \simeq \frac{\bar{s}\bar{s}\bar{d}}{ssd} = \lambda_s^{-4}(\lambda_u\lambda_d)^{-1} = e^{4\mu_S/T} e^{-2\mu_B/T}, \quad (37)$$

lead to a very good estimate of the baryochemical potential and strange chemical potential, and thus, to predictions of other particle ratios [9].

The sensitivity of particle yields to phase space occupancy factors γ_i derives from comparison of hadron yields with differing q, s quark content, e.g.:

$$\frac{\Xi^-(dss)}{\Lambda(uds)} \propto \frac{\gamma_d\gamma_s^2}{\gamma_u\gamma_d\gamma_s} \frac{g_\Xi\lambda_d\lambda_s^2}{g_\Lambda\lambda_u\lambda_d\lambda_s}, \quad \frac{\bar{\Xi}^-(\bar{d}\bar{s}\bar{s})}{\bar{\Lambda}(\bar{u}\bar{d}\bar{s})} \propto \frac{\gamma_d\gamma_s^2}{\gamma_u\gamma_d\gamma_s} \frac{g_\Xi\lambda_d^{-1}\lambda_s^{-2}}{g_\Lambda\lambda_u^{-1}\lambda_d^{-1}\lambda_s^{-1}}. \quad (38)$$

In Eq. (38), each of the ratios also contain chemical potential factors λ_i . These can be eliminated by taking the product of particle ratio with antiparticle ratio, thus,

$$\frac{\Xi^-(dss)}{\Lambda(uds)} \frac{\bar{\Xi}^-(\bar{d}\bar{s}\bar{s})}{\bar{\Lambda}(\bar{u}\bar{d}\bar{s})} = C_{\Xi\Lambda}^2 \left(\frac{\gamma_s}{\gamma_u} \frac{g_\Xi}{g_\Lambda} \right)^2, \quad \frac{\Lambda(uds)}{p(uud)} \frac{\bar{\Lambda}(\bar{u}\bar{d}\bar{s})}{\bar{p}(\bar{u}\bar{u}\bar{d})} = C_{\Lambda p}^2 \left(\frac{\gamma_s}{\gamma_u} \frac{g_\Lambda}{g_p} \right)^2. \quad (39)$$

The proportionality constant C_{ab} describes the phase space size ratio for the two particles a, b of different mass. It incorporates the contributions from resonance decays, which of course differ from particle to particle.

The method applied in Eq. (39) can be used in several other such double particle ratios. The relevance of this is that we have identified an experimental observable (combination of particle ratios) solely dependent on two parameters of statistical hadronization and chemical freeze-out, the temperature T which controls the phase space factor ratio C and the occupancy ratio γ_s/γ_q . The two ratios shown in Eq. (39)), allow to constrain the value of γ_s/γ_q only as function of T . Other such ratios are available. Some, e.g., made of mesons, in general, will be weakly dependent on chemical potentials since some kaons and pions are decay products of baryonic resonances. For this reason, it is more appropriate to study a global fit to the data. However, considerations as presented here, show better which data is important and contains the type of information we are seeking to determine.

Pursuing this further, we note that the most difficult to extract, even in a qualitative manner, from the data is the value of the parameter γ_q . One recognizes easily that the yield of baryons is proportional to $V\gamma_q^3(\gamma_s/\gamma_q)^{n_s}$, where n_s is the total number of constituent strange quarks or anti-quarks. Similarly, we note that the yield of mesons is proportional to $V\gamma_q^2(\gamma_s/\gamma_q)^{n_s}$. Thus, ratio of baryons to mesons at fixed value of γ_s/γ_q is the sole source of information on γ_q . What we see is also that γ_q allows us to increase the yield of baryons compared to the yield of mesons. This is a very important feature in statistical hadronization, considering that microscopic pictures of quark recombination provide yields of baryons and mesons which do not follow the chemical equilibrium distributions, and especially at RHIC are quite different such expectations.

Some argue that T can fulfill the function of tuning relative meson to baryon ratio as well. However, in general, T has to produce the right resonance yield and should not be manipulated to balance baryon to meson yield. A consequence of setting $\gamma_q = 1$ is that the overall ratio of baryons to mesons fixes the value of T and thus there ensues a failure in description of resonance yields — this in turn creates an (as we believe redundant) industry of resonance evolution studies. Despite this effort, there is no consistent model which starts with $\gamma_q = 1$ and can describe both stable particles and resonance yields. Those who pursue this approach must at least briefly consider the fact that, in their model, the resonance results remain unexplained. This in turn means that their use of SHM is totally internally inconsistent since the yields of all particles, as we have seen, depend decisively on resonance yields. Add to these remarks, the fact that when $\gamma_q \neq 1$ one finds fits of data which are quite much better than for $\gamma_q = 1$.

4.2 Energy Scan at CERN-SPS

4.2.1 Global data analysis

When facing a large data sample, with many particle yields presented at different energies, it is better to perform a global fit of statistical parameters, rather than to focus on a subset of data such as resonances or hyperon ratios. In that way a proper weighting of all errors is arrived at, with the resulting parameter set applying to all data at the same time. As already noted the public statistical hadronization program, SHARE has simplified this task considerably [11,12]. As an example of the prevailing situation I will consider here the SPS data set of NA49 [47], the experiment in which József Zimányi participated. The SPS data is complemented with the highest energy AGS data to show that the low energy anomaly we find is present both at SPS lowest energy (20 A GeV) and top AGS energy (11 A GeV), with different experimental set-up and accelerators involved. thus the outcome we find is very likely not data but model and analysis method related. For the method we refer to the detailed presentation of the analysis of the top energy AGS results see Ref. [48].

The outcome of the fit procedure is stated in the top section of table 2. The λ_s values, marked with an asterisk * in table 2, are result of a strangeness conservation constraint, which, however, is not chosen to be zero, but as shown in table: since strangeness conservation constraint involves several particle yields it is inappropriate to insist on $s - \bar{s} = 0$, for this correlates the errors of the input data, which are experimentally not correlated. Our procedure was to fit first without strangeness conservation, and once we see the strangeness asymmetry to fix it at a reasonable

Table 2. For each projectile energy E [A GeV] for AGS and SPS energy range, we present in the header $\sqrt{s_{NN}}$, the invariant center of momentum energy per nucleon pair, y_{CM} the center of momentum rapidity. This is followed by statistical parameters T, λ_i, γ_i obtained in the fit, the strangeness asymmetry required, and we present the resulting chemical potentials μ_B, μ_S , the reaction volume V and the centrality of the reaction considered. This is followed first by input and then by output total hadron multiplicity $N_{4\pi}$.

E [A GeV]	11.6	20	30	40	80	158
$\sqrt{s_{NN}}$ [GeV]	4.84	6.26	7.61	8.76	12.32	17.27
y_{CM}	1.6	1.88	2.08	2.22	2.57	2.91
T [MeV]	157.8 \pm 0.7	153.4 \pm 1.6	123.5 \pm 3	129.5 \pm 3.4	136.4 \pm 0.1	136.4 \pm 0.1
λ_q	5.23 \pm 0.07	3.49 \pm 0.08	2.82 \pm 0.08	2.42 \pm 0.10	1.94 \pm 0.01	1.74 \pm 0.02
γ_q	0.335 \pm 0.006	0.48 \pm 0.05	1.66 \pm 0.10	1.64 \pm 0.04	1.64 \pm 0.01	1.64 \pm 0.001
γ_s	0.190 \pm 0.009	0.38 \pm 0.05	1.84 \pm 0.32	1.54 \pm 0.15	1.54 \pm 0.05	1.61 \pm 0.02
λ_{f3}	0.877 \pm 0.116	0.863 \pm 0.08	0.939 \pm 0.023	0.951 \pm 0.008	0.973 \pm 0.002	0.975 \pm 0.004
λ_s	1.657*	1.41*	1.36*	1.30*	1.22*	1.16*
$s - \bar{s}/s + \bar{s}$	0	-0.092	-0.085	-0.056	-0.029	-0.062
μ_B [MeV]	783	576	384	344	271	227
μ_S [MeV]	188	139	90.4	80.8	63.1	55.9
V [fm ³]	3596 \pm 331	4519 \pm 261	1894 \pm 409	1879 \pm 183	2102 \pm 53	3004 \pm 1
$N_{4\pi}$ centrality	most central	7%	7%	7%	7%	5%
$R = p/\pi^+, N_W$	$R = 1.23 \pm 0.13$	349 \pm 6	349 \pm 6	349 \pm 6	349 \pm 6	362 \pm 6
Q/b	0.39 \pm 0.02	0.394 \pm 0.02	0.394 \pm 0.02	0.394 \pm 0.02	0.394 \pm 0.02	0.39 \pm 0.02
π^+	133.7 \pm 9.9	184.5 \pm 13.6	239 \pm 17.7	293 \pm 18	446 \pm 27	619 \pm 48
$R = \pi^-/\pi^+, \pi^-$	$R = 1.23 \pm 0.07$	217.5 \pm 15.6	275 \pm 19.7	322 \pm 19	474 \pm 28	639 \pm 48
$R = K^+/K^-, K^+$	$R = 5.23 \pm 0.5$	40 \pm 2.8	55.3 \pm 4.4	59.1 \pm 4.9	76.9 \pm 6	103 \pm 10
K^-	3.76 \pm 0.47	10.4 \pm 0.62	16.1 \pm 1	19.2 \pm 1.5	32.4 \pm 2.2	51.9 \pm 4.9
$R = \phi/K^+, \phi$	$R = 0.025 \pm 0.006$	1.91 \pm 0.45	1.65 \pm 0.5	2.5 \pm 0.25	4.58 \pm 0.2	7.6 \pm 1.1
Λ	18.1 \pm 1.9	28 \pm 1.5	41.9 \pm 6.1	43.0 \pm 5.3	44.7 \pm 6.0	44.9 \pm 8.9
$\bar{\Lambda}$	0.017 \pm 0.005	0.16 \pm 0.03	0.50 \pm 0.04	0.66 \pm 0.1	2.02 \pm 0.45	3.68 \pm 0.55
Ξ^-		1.5 \pm 0.13	2.48 \pm 0.19	2.41 \pm 0.39	3.8 \pm 0.260	4.5 \pm 0.20
Ξ^+			0.12 \pm 0.06	0.13 \pm 0.04	0.58 \pm 0.13	0.83 \pm 0.04
$\Omega + \bar{\Omega} // K_S$				0.14 \pm 0.07		81 \pm 4
$b \equiv B - \bar{B}$	375.6	347.9	349.2	349.9	350.3	362.0
π^+	135.2	181.5	238.7	290.0	424.5	585.2
π^-	162.1	218.9	278.1	326.0	461.3	643.9
K^+	17.2	39.4	55.2	56.7	77.1	109.7
K^-	3.58	10.4	15.7	19.6	35.1	54.1
K_S	10.7	25.5	35.5	37.9	55.1	80.2
ϕ	0.46	1.86	2.28	2.57	4.63	7.25
p	174.6	161.6	166.2	138.8	138.8	144.3
\bar{p}	0.021	0.213	0.68	0.76	2.78	5.46
Λ	18.2	29.7	39.4	34.9	42.2	48.3
$\bar{\Lambda}$	0.016	0.16	0.51	0.63	2.06	4.03
Ξ^-	0.47	1.37	2.44	2.43	3.56	4.49
Ξ^+	0.0026	0.027	0.089	0.143	0.42	0.82
Ω	0.013	0.068	0.14	0.144	0.27	0.38
$\bar{\Omega}$	0.0008	0.0086	0.022	0.030	0.083	0.16
$K^0(892)$	5.42	13.7	11.03	12.4	18.7	26.6
Δ^0	38.7	33.43	25.02	26.6	27.2	28.2
Δ^{++}	30.6	25.62	22.22	24.2	25.9	26.9
$\Lambda(1520)$	1.36	2.06	1.73	1.96	2.62	2.99
$\Sigma^-(1385)$	2.51	3.99	4.08	4.26	5.24	5.98
$\Xi^0(1530)$	0.16	0.44	0.69	0.73	1.14	1.44
η	8.70	16.7	19.9	24.1	38.0	55.2
η'	0.44	1.14	1.10	1.41	2.52	3.76
ρ^0	12.0	19.4	14.0	18.4	32.1	42.3
$\omega(782)$	6.10	13.0	10.8	15.7	27.0	38.5
$f_0(980)$	0.56	1.18	0.83	1.27	2.27	3.26

nett value shown in table so that there is no spurious constraint introduced among strange hadrons due to independent measurement, yet there is some input of the fact that strangeness is produced in pairs.

The profiles of χ^2 , and of the confidence level $P[\%]$ determining the fit quality are shown in Fig. 7. I note that the results for AGS 11.6 and SPS 20 GeV differ from the remainder of the SPS results (30, 40, 80 and 158 GeV) in the outcome of the fit. The low energy results, obtained at two different experimental locations, clearly favor a value of $\gamma_q < 1$, combined with relatively

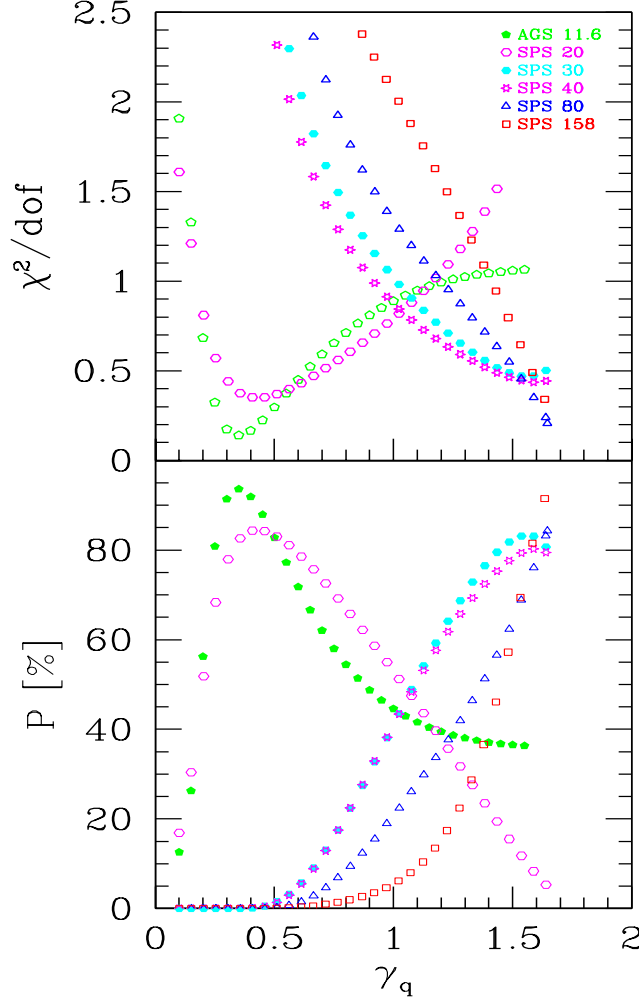


Fig. 7. χ^2/dof (top) and the associated confidence level $P[\%]$ (bottom) as function of γ_q , the light quark phase space occupancy. for the AGS/SPS energy range.

large V, T , while the higher energy data favor $\gamma_q \rightarrow \gamma_q^{\text{cr}} \simeq 1.6$. Inspecting, in particular, the 80 and 158 GeV profiles, presented in Fig. 7, we recognize that the semi-equilibrium model with $\gamma_q = 1$ has a comparatively low viability compared to the full chemical non-equilibrium model we advance. Thus the recent increase in NA49 data sample has tilted the preference strongly to the full chemical non-equilibrium interpretation of the data.

In passing I have to stress that for the present SPS data these fits are very stable. There is a clear unique best fit. We trace back this to the fact that the number of participants (both protons and neutrons) is prescribed by the trigger condition. Leaving this input out generates instability, as does ad-hoc approach to charge (isospin) asymmetry - to best of my knowledge only SHARE offers at present the correct evaluation of λ_3 parameter which controls charge asymmetry, and is of particular importance in the study of SPS/AGS data.

The SHARE package offers further the opportunity using the statistical parameters to evaluate the physical properties of the fireball in its local frame of reference: since we look at the hadron yields, the flow velocity information is not retained. Some of these results are shown in table 3. We note that the chemical freeze-out at low energy (AGS 11.6 and SPS 20 GeV) occurs from a much more dilute physical state, the energy density of the high energy (30, 40, 80 and 158 GeV) data points hovers well above 400–500 MeV/fm³, about a factor 2.5 higher

Table 3. The physical properties. Top: pressure P , energy density $\epsilon = E_{\text{th}}/V$, entropy density S/V , for AGS and CERN energy range at, (top line) projectile energy E [GeV]; middle: dimensionless ratios of properties at fireball breakup, E_{th}/TS ; strangeness per entropy s/S , strangeness per baryon s/b ; and bottom the fraction of initial collision energy in thermal degrees of freedom, $(2E_{\text{th}}/b)/\sqrt{s_{\text{NN}}}$, the energy cost to make strangeness pair E_{th}/\bar{s} , thermal energy per hadron at hadronization E_{th}/h .

$E[A\text{GeV}]$	11.6	20	30	40	80	158
$\sqrt{s_{\text{NN}}} [\text{GeV}]$	4.84	6.26	7.61	8.76	12.32	17.27
$P[\text{MeV}/\text{fm}^3]$	21.9	21.3	58.4	68.0	82.3	76.9
$\epsilon[\text{MeV}/\text{fm}^3]$	190.1	166.3	429.7	480.2	549.9	491.8
$S/V[1/\text{fm}^3]$	1.25	1.21	2.74	3.07	3.54	3.26
E_{th}/TS	0.96	0.92	1.27	1.20	1.14	1.11
$100\bar{s}/S$	0.788	1.26	1.94	1.90	2.16	2.22
\bar{s}/b	0.095	0.202	0.289	0.314	0.459	0.60
$(2E_{\text{th}}/b)/\sqrt{s_{\text{NN}}}$	0.752	0.722	0.612	0.589	0.536	0.472
$E_{\text{th}}/\bar{s} [\text{GeV}]$	19.25	10.9	8.08	8.21	7.19	6.80
$E_{\text{th}}/h [\text{GeV}]$	1.33	1.18	0.866	0.859	0.827	0.766

than at low energy. Errors on these results can be studied by evaluating a profile of χ^2 varying a fixed value of for example P . This shows that the errors are at the level of 6% for extensive quantities P, ϵ, S . Thus clearly confirms that the difference between these two groups of results is physical.

I find that between 20 and 30 GeV the ratio E/TS shifts from a value below unity, to above unity, as is required for the sudden, supercooled hadronization mechanism expected to operate for $E > 20 A$ GeV. There is a steady growth in the yield of strangeness, both measured in terms of s/S as well as the yield per participant (net baryon number b). There is a decrease in the energy retained, indicating that the flow effects grow rapidly, pushing the fraction of energy stopping below 50% at the top SPS energy. The cost of strangeness pair production E_{th}/\bar{s} decreases, as does the energy per hadron produced E_{th}/h . Both these quantities use energy content in the local rest frame, and thus do not include the kinetic energy of matter flow at hadronization, which originated from the thermal pressure, and which has driven the expansion matter flow.

4.2.2 Discussion of fit results

At the top SPS energy, the value of $s/S = 0.022$ implies for a QGP source a $\gamma_s^Q \simeq 0.7$, which corresponds to $\gamma_s/\gamma_q \simeq 1$. This, in fact, is the reason why chemical equilibrium $\gamma_q = \gamma_s = 1$ ‘marginally works’ for this data set. However, as function of energy we see a very spectacular preference for non-equilibrium, of two different types. For two lowest reaction energies considered, the results are below chemical equilibrium and for other, higher energies, with $\sqrt{s_{\text{NN}}} > 7.6$ GeV there is over saturation of chemical occupancies.

The data are fit very well, and thus also describe precisely the K^+/π^+ ratio as we show in Fig. 8. This result has been one of major challenges which other groups have failed to understand. The maximum of the ratio K^+/π^+ occurs for $E = 30 A$ GeV where I find $\gamma_i > 1$. An anomaly associated with the horn is the large yield of Λ , and protons, see bottom section of table 2. I further note that the structure of the horn shown by dashed (semi-equilibrium) and dotted (equilibrium) lines is also reproduced qualitatively, contrary to results of other groups. This behavior is due to the relaxation of the strangeness conservation condition, which as discussed above cannot be imposed stringently, seen that measurement errors are not correlated.

It has been argued [49] that the hadronization condition is defined by the energy available per primary hadron E/h_p . Using SHARE the results shown in Fig. 9 by triangles arise, dashed

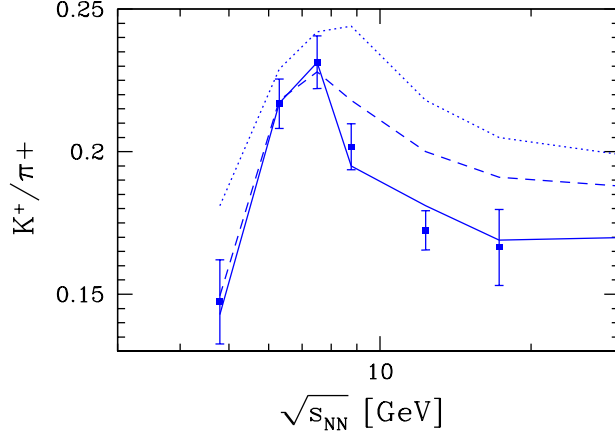


Fig. 8. K^+/π^+ total yields as function of $\sqrt{s_{NN}}$. The solid lines show chemical non-equilibrium model fit. The chemical equilibrium fit result is shown by the dotted line. The dashed line arises finding best γ_s for $\gamma_q = 1$.

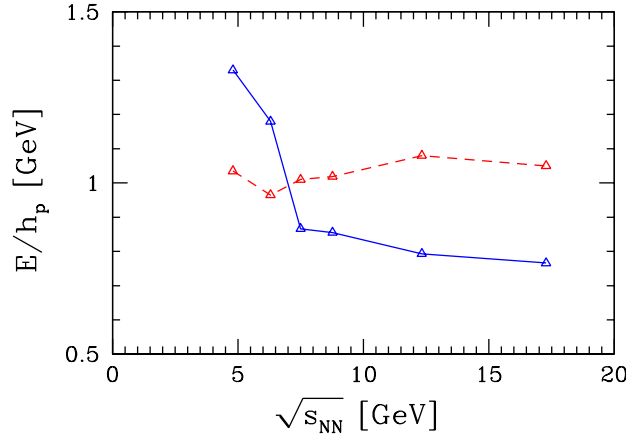


Fig. 9. E/h_p ratio of the thermal energy of the fireball with total number of primary hadrons, prior to strong decays as function of reaction energy $\sqrt{s_{NN}}$. Solid line (blue) connect results for chemical non-equilibrium, dashed line (red) connect results for semi-equilibrium with $\gamma_q = 1$.

(red) connecting lines indicate results assuming $\gamma_q = 1$. The solid (blue) line connect results presented here, with $\gamma_q \neq 1$. We see that there is a strong dependence of E/h_p on chemical equilibration conditions at freeze-out: $E/h_p(\gamma_q, \gamma_s)$, while the main dependence on T, μ_b (nearly) cancels, a feature of considerable interest, but not at all *alone* controlling the hadronization process. On the other hand this near cancellation of T, μ_b dependence is a silent feature allowing to stabilize the search for the true physical fit of hadronization data in a highly multidimensional approach which includes all chemical parameters. We will return in near future to discuss this in depth [51]. It is further interesting to note that the energy cost to produce strangeness seen in table 3 is higher, roughly by a factor π/K .

Do the low energy results imply absence of quark matter, and thus reactions between individual hadrons? Our analysis shows that the chemical freeze-out occurs in a highly dilute phase. However, the rapid rise of strangeness yield as function of reaction energy, suggests that the strangeness production processes differ from those encountered in normal hadron matter. For this reason we favor a constituent quark matter reaction picture at 11.6 and 20 A GeV,

with color deconfinement arising yet below this energy range. The relatively high temperature and low γ_q are consistent with properties of constituent quark phase with $m_{u,d} \simeq 340$ MeV and $m_s \simeq 500$ MeV, gluons are ‘frozen’. In such a massive deconfined quark phase chiral symmetry is not restored. For $\mu_B \rightarrow 0$ the lattice results unite the chiral symmetry restoration, in which $m_q \rightarrow 0$, with the deconfinement transition.

In Summary: the physical properties we find for the hadronization of 30, 40, 80, 158 A GeV most central heavy ion reactions correspond to the expected behavior of the chirally symmetric QGP phase. SHM model described these results well, hadron simulations (not discussed here) fail to account for multistrange (anti)baryons. 11 and 20 A GeV hadronization is different, and importantly the results from AGS and SPS lead to the same different results. What exactly happens, and if, in particular sudden hadronization applies in this energy domain is discussed in some more detail in another work [50], and requires further study.

5 Unde venimus, Ubi sumus, Quo vadis

5.1 From quarks in hadrons to quark-gluon matter

Modern subatomic physics cannot exist without quarks, yet these particles have never been seen individually. The introduction of a dynamical model of strong interactions [52], created a vast new field of study, the structured QCD vacuum. Confinement of quarks is interpreted as a feature of the color frozen vacuum state in which we live. When in early Universe at about $30\mu s$, the ambient temperature dropped below hadronization condition, the quark Universe froze and turned into hadrons. The early hot Universe did not confine quarks.

The idea to recreate the quark Universe in the laboratory collisions of large nuclei presupposes that in principle it is possible to embed a small spatial region of melted, deconfined vacuum in the global frozen vacuum. That this is an issue is due to Lorentz/Poincare symmetry, which restricts us to a unique vacuum state. However, in order to heat the vacuum, we crash matter locally, which breaks the Poincare symmetry, allowing to consider two different forms of the Lorentz invariant “ether” at the same time. That this is possible is not entirely compelling to everyone. Moreover, there is a time constant of vacuum melting, and I wish to know its value! If the melting in the conditions of heavy ion collisions is too slow, the confined state remains. Thus formation of QGP is not assured, even though there is a general consensus that it does not contradict principles of physics, or cumulative knowledge about the standard model, and hadron structure.

Considering that a nucleon has a hadronic radius of about $R_N = 1$ fm, and the much greater u, d quark Compton wavelength $\lambda_{u,d} = h/m_{u,d}c > 100R_N$, quark repulsion by the ‘frozen’ vacuum is required to understand hadron structure. The ‘inside’ of a hadron is an excited state of the frozen vacuum. One could easily think this is similar to QGP vacuum. However, it is impossible to construct a model with volume energy above 200 MeV/fm^3 . Yet the study of QCD on the lattice requires that latent heat of deconfinement is at the level of 500 MeV/fm^3 . Thus there must be not one but at least two different vacuum states aside of quark-empty frozen vacuum around us:

- a) ‘half-vacuum’ which tolerates quarks, but no gluons and is found inside the normal hadron;
- b) ‘perturbative thermal QCD vacuum’ which comprises mobile gluons and is called QGP.

I still do not quite understand how to freeze gluons without freezing quarks. Yet, this must be possible in presence of relatively high quark density, for not too high temperatures.

What I want to make sure everyone who read this report to this point recognizes that colliding heavy ions can form two thresholds of new phases. We must be prepared to see mobility (deconfinement) of effectively massive quarks at relatively low excitation energy. Only after quarks turn mass less, the chiral symmetry is restored, perturbative gluon degrees of freedom should be present, and the quark-gluon plasma phase develops. All this also involves as noted above the time constant of the vacuum melting which can obscure the two or more phase thresholds. Our analysis of data suggests that this valon (for valance) quark phase could be present at highest AGS energies, and lowest SPS energy range. The valon semi-relativistic quark matter most resembling squashed nucleons is possibly present in the center of collapsed stars.

Such a state of matter will be quite different from the hot QGP state formed with great certainty in the RHIC and soon LHC environments. As noted the latent phase heat of this phase could be different by about a factor 5-10 from QGP-HG latent heat. Thus there is need to develop and consider two different intuitive descriptions of deconfined matter, one valid at high temperature and low baryon density (QGP) and the other at (relatively) low temperature and high baryon density (dense quark matter). This alternate quark matter state has had a long history [53], yet only recently there has been a surge of interest [54].

5.2 Strangeness from AGS to LHC

In order to study the properties of phases of hadronic matter formed in relativistic heavy ion collisions, I presented a two step procedure:

- a) A model (SHM-SHARE) is developed which allows to *reliably* describe the observed particle yields, and thus to extrapolate to unobserved phase space domains, or particle types.
- b) Using all particle yields and the statistical parameters we can compute the physical properties of the source.

In this way we obtain a snap shot of the hot matter fireball, taken at the time of particle chemical freeze-out. Much effort in this report was devoted to explain why I chase a reliable data fit with high confidence level: only if this is well accomplished, I have a reliable extrapolation of the unobserved particle yields, required for precise description of the physical properties of the fireball, and I can trust the viability of these results.

Looking at the snap shot seen in table 3 I note that there is an reaction energy threshold which indicates onset of the formation of the perturbative state of QGP near to 30 A GeV. Interestingly, the rate of growth of strangeness yield as function of the rate of growth in the reaction energy diminishes at this point, which is seen as a knee in some particle yields/ratios. Since the rate of growth in entropy (pions) is faster than strangeness, there appears a ‘horn’ structure in K^+/p_i^+ ratio, shown in Fig. 8

Looking at the rapid rise of strangeness yield \bar{s}/b in table 3 at and below 30 A GeV I recognize that the production of strangeness is rising faster at low reaction energy, in the valon-type quark matter which we probably encounter at the top AGS and bottom SPS energy range. Among factors helping to explain this is:

- a) at lower reaction energy stopping of matter and energy is more effective and thus available thermal energy is much greater, which is important considering as is seen in table 3 the energy cost of strangeness production. There is a rather sudden drop in stopping between 20 A GeV and 30 A GeV (see 3rd last entry line in table 3).
- b) the more dilute hadronization condition implies a longer expansion lifespan.
- c) the higher temperature profile of this phase – massive u, d -valons are above threshold for strangeness-valon production at all times.

The availability of the yields of multistrange hadrons, and of resonances allows to confirm the chemical nonequilibrium (sudden) hadronization picture for the QGP range of reaction energies (at and above 30 A GeV). Assuming HG phase space chemical equilibrium is simply not a reasonable model to follow when fitting the data, even if when only looking at the value $\gamma_q = 1$ in Fig. 7 the totality of fits seems to be reasonable there. Only in the nonequilibrium model can the systematic of (multi)strange hadron production as function of reaction energy be described consistently. The horn, Fig. 8, shows this, as do similar results for other particles. I note several important roles the parameter γ_q must fulfill:

- a) balance entropy in a fast transition of an entropy rich QGP to an entropy poor hadron phase;
- b) shift the relative yield of mesons and baryons appropriate for combinant hadronization yields;
- c) correct for imperfections in the understanding and/or use of hadron spectra.

Regarding the last point I note that it cannot be expected that the empirical baryon and meson spectra which enter the SHM are completely understood. γ_q fudges the incomplete knowledge. Conversely, ad-hock assumption of a value expected in perfect world, viz. chemical hadron equilibrium $\gamma_q = 1$ presumes also that the SHM model as used is completely understood.

It is appropriate to close the discussion noting that the theoretical computation of strangeness production based on gluon fusion in QGP matches analysis results for \bar{s}/b and \bar{s}/S seen

in table 3. According to the model calculations presented this rise of the production continues through the RHIC energy range reaching much higher (nearly double SPS) values of \bar{s}/S at LHC. Thus yields of strange hadrons at LHC will be further out of chemical equilibrium, with relatively large γ_s expected. For $K^+/p\pi^+$ this means that we reach back to, and above the peak of the horn at LHC. For multi-strange hyperons, and the ϕ , this implies substantially increased rapidity yields dN/dy .

Credits

I wish to thank the students of József Zimányi: Tamás Bíró, Tamás Csorgo and Peter Levai for their seminal work addressing the reaction dynamics in heavy ion collisions, and quark–gluon plasma which helped to shape my understanding of the subject, and for the very stimulating and informative meeting offering a deeper insight about profound accomplishments of József Zimányi. Comments I received from Tamás Bíró, Peter Levai and Jean Letessier and an unnamed referee about this elucidation of hadron chemistry have greatly improved my presentation and the ability to communicate and explain. I thank my friends, students, and collaborators who published with me the insights here presented, and in particular, (in alphabetical order) Peter Koch, Inga Kuznetsova, Jean Letessier, Berndt Müller and Giorgio Torrieri.

Support Acknowledgment

Work supported by a grant from: the U.S. Department of Energy DE-FG02-04ER4131.

Reference Remark

This is not a review paper of a vast field of knowledge but a personal account of the work pertinent to an important period in life and work of József Zimányi. For this reason work most appropriate for this occasion appears below. I apologize to all colleagues whose work has not been mentioned.

References

1. J. Rafelski and R. Hagedorn, “From Hadron Gas To Quark Matter. 2,” in *Statistical Mechanics of Quarks and Hadrons*, H. Satz, ed. (Norht Holland 1980) pp. 253–272, also: Preprint CERN-TH-2969, October 1980.
2. T. Biro and J. Zimanyi, Phys. Lett. B **113** (1982) 6, also preprint KFKI-1981-69.
3. B. L. Combridge, Nucl. Phys. B **151** (1979) 429.
4. B. Muller and J. Rafelski, Phys. Lett. B **101** (1981) 111.
5. J. Rafelski and B. Muller, Phys. Rev. Lett. **48** (1982) 1066 [Erratum-ibid. **56** (1986) 2334].
6. P. Koch and J. Rafelski, Nucl. Phys. A **444** (1985) 678.
7. P. Koch, B. Muller and J. Rafelski, Phys. Rept. **142** (1986) 167.
8. T. S. Biro, P. Levai and J. Zimanyi, Phys. Lett. B **347** (1995) 6.
9. J. Rafelski, Phys. Lett. B **262** (1991) 333.
10. J. Letessier and J. Rafelski, Int. J. Mod. Phys. E **9** (2000) 107 [arXiv:nucl-th/0003014].
11. G. Torrieri, S. Steinke, W. Broniowski, W. Florkowski, J. Letessier and J. Rafelski, Comput. Phys. Commun. **167** (2005) 229 [arXiv:nucl-th/0404083].
12. G. Torrieri, S. Jeon, J. Letessier and J. Rafelski, Comput. Phys. Commun. **175** (2006) 635 [arXiv:nucl-th/0603026].
13. F. Becattini and G. Passaleva, Eur. Phys. J. C **23** (2002) 551 [arXiv:hep-ph/0110312].
14. P. Koch, J. Rafelski and W. Greiner, Phys. Lett. B **123** (1983) 151.
15. T. Csorgo, J. Phys. Conf. Ser. **50** (2006) 259 [arXiv:nucl-th/0505019].

16. W. Florkowski, W. Broniowski, A. Kisiel and J. Pluta, *Acta Phys. Polon. B* **37** (2006) 3381 [arXiv:nucl-th/0609054].
17. J. Letessier, J. Rafelski and A. Tounsi, *Phys. Rev. C* **50** (1994) 406 [arXiv:hep-ph/9711346].
18. J. Rafelski and J. Letessier, *Eur. Phys. J. C* **45** (2006) 61 [arXiv:hep-ph/0506140].
19. I. Kuznetsova and J. Rafelski, *Eur. Phys. J. C* **51** (2007) 113 [arXiv:hep-ph/0607203].
20. J. Alam, B. Sinha and S. Raha, *Phys. Rev. Lett.* **73**, 1895 (1994).
21. R. Hamberg, W. L. van Neerven and T. Matsuura, *Nucl. Phys. B* **359** (1991) 343 [Erratum-ibid. B **644** (2002) 403].
22. N. Kidonakis and R. Vogt, *Eur. Phys. J. C* **36** (2004) 201 [arXiv:hep-ph/0401056].
23. J. Rafelski, *Phys. Rept.* **88** (1982) 331.
24. R. J. Glauber, *Nucl. Phys. A* **774** (2006) 3 [arXiv:nucl-th/0604021], and references therein.
25. A. Bialas, M. Bleszynski and W. Czyz, *Nucl. Phys. B* **111** (1976) 461.
26. F. Antinori *et al.* [WA97/NA57 Collaboration], *Nucl. Phys. A* **661** (1999) 357, *Eur. Phys. J. C* **18** (2000) 57, *J. Phys. G* **32** (2006) 427 [arXiv:nucl-ex/0601021].
27. P. Castorina, D. Kharzeev and H. Satz, *Eur. Phys. J. C* **52** (2007) 187 [arXiv:0704.1426 [hep-ph]].
28. A. Tounsi, A. Mischke and K. Redlich, *Nucl. Phys. A* **715** (2003) 565 [arXiv:hep-ph/0209284].
29. J. Rafelski and M. Danos, *Phys. Lett. B* **97**, 279 (1980).
30. I. Kraus, J. Cleymans, H. Oeschler, K. Redlich and S. Wheaton, *Phys. Rev. C* **76**, 064903 (2007) [arXiv:0707.3879 [hep-ph]].
31. A. Dainese [NA57 Collaboration], *Nucl. Phys. A* **774** (2006) 51 [arXiv:nucl-ex/0510001].
32. F. Becattini, J. Manninen and M. Gazdzicki, *Phys. Rev. C* **73** (2006) 044905 [arXiv:hep-ph/0511092].
33. H. Caines, *J. Phys. G* **32**, S171 (2006) [arXiv:nucl-ex/0608008].
34. R. Hagedorn, *Nuovo Cim. Suppl.* **3** (1965) 147.
35. J. Rafelski, J. Letessier and G. Torrieri, *Phys. Rev. C* **64** (2001) 054907 [Erratum-ibid. C **65** (2002) 069902] [arXiv:nucl-th/0104042].
36. G. Torrieri and J. Rafelski, *Phys. Lett. B* **509** (2001) 239 [arXiv:hep-ph/0103149].
37. M. Bleicher and H. Stoecker, *J. Phys. G* **30** (2004) S111 [arXiv:hep-ph/0312278].
38. C. Markert, *Eur. Phys. J. C* **49** (2007) 125.
39. J. Adams *et al.* [STAR Collaboration], *Phys. Rev. Lett.* **97** (2006) 132301 [arXiv:nucl-ex/0604019].
40. S. Salur, *J. Phys. G* **32** (2006) S469 [arXiv:nucl-ex/0606002].
41. J. Zimanyi and P. Levai, *Acta Phys. Hung. A* **27** (2006) 469 [arXiv:nucl-th/0404060].
42. G. Torrieri and J. Rafelski, *Phys. Rev. C* **75** (2007) 024902 [arXiv:nucl-th/0608061].
43. T. Csorgo and L. P. Csernai, *Phys. Lett. B* **333** (1994) 494 [arXiv:hep-ph/9406365].
44. L. P. Csernai and I. N. Mishustin, *Phys. Rev. Lett.* **74** (1995) 5005.
45. T. S. Biro, P. Levai and J. Zimanyi, *Phys. Rev. C* **59** (1999) 1574 [arXiv:hep-ph/9807303].
46. J. Rafelski and J. Letessier, *Phys. Rev. Lett.* **85** (2000) 4695 [arXiv:hep-ph/0006200].
47. The results of NA49 we use were provided by M. Gazdzicki and B. Lungwitz, (private communication, September 2006)
48. J. Letessier, J. Rafelski and G. Torrieri, arXiv:nucl-th/0411047.
49. J. Cleymans and K. Redlich, *Phys. Rev. Lett.* **81** (1998) 5284 [arXiv:nucl-th/9808030].
50. J. Letessier and J. Rafelski, arXiv:nucl-th/0504028.
51. M. Petran, J. Letessier and J. Rafelski, *Centrality Dependence of Hadronization Condition at RHIC* in preparation.
52. H. Fritzsch, M. Gell-Mann and H. Leutwyler, *Phys. Lett. B* **47** (1973) 365.
53. B. C. Barrois, *Nucl. Phys. B* **129** (1977) 390.
54. M. G. Alford, A. Schmitt, K. Rajagopal and T. Schafer, "Color superconductivity in dense quark matter," submitted to *Rev. Mod. Phys.*, arXiv:0709.4635 [hep-ph].